

An Investigation into Halbach-Based Planar Magnetic Drivers as a Viable Alternative to Traditional Headphone Designs

Third Year Individual Project – Final Report

Date of submission

April 2025

Shay Campbell

11079275

Supervisor:

Cheng Zhang

School of Engineering

Contents

Contents	2
Abstract	4
Declaration of originality	5
Intellectual property statement	6
1 Introduction	7
1.1 Background	7
1.2 Motivation	7
1.3 Aims and Objectives	8
1.4 Report Structure	9
2 Literature Review	9
2.1 Types of driver technology	9
3 Methodology	14
3.1 Theoretical Development	14
3.2 PCB Optimisation	17
3.3 Permanent magnet array optimisation	21
4 Design and Implementation	22
4.1 Permanent Magnet Design	22
4.2 PCB Design	29
5 Experiment results	32
6 Discussion	34
6.1 Planar Magnetic Headphone (Custom System)	34
6.2 Sony WH-1000XM3 Benchmark Comparison	37
7 Conclusion and Future Works	40
A Appendices	44
A.1 Project Outline	44
A.2 Initial Project Plan	45
A.3 Risk Register	46
A.4 Continued Professional Development	46

A.5	Health & Safety Risk Assessment	47
A.6	Gantt Chart	50
A.7	Source Code	50

Word count: 10936

Abstract

Despite yearly advancements in headphone technology, consumers still face compromises when choosing a device, typically between sound quality and portability, often sacrificing one for the other or paying a premium to achieve both. Studio-grade audio usually comes with added weight and bulk, while mainstream products prioritise convenience at the expense of fidelity. This thesis explores a solution to this trade-off by introducing a novel implementation of planar magnetic technology that delivers both high-quality audio and portability in a single form factor. The design features a flexible diaphragm embedded with serpentine copper traces, suspended between two Halbach magnet arrays. This configuration enables precise diaphragm movement, allowing accurate and detailed sound reproduction with minimal distortion. Performance was evaluated by assessing the system's ability to reproduce a reference signal consistently and accurately. Results showed a mostly resistive load with only 0.6Ω of impedance variation across the audible range, resulting in minimal signal colouration. Compared to a commercial benchmark (Sony WH-1000XM3), the system demonstrated an 88% reduction in diaphragm impedance variation and improved voltage linearity. Additionally, it achieved a lower weight than typical planar magnetic headphone designs. User feedback confirmed that the prototype delivers clear, high-resolution audio in a comfortable and lightweight form. Future improvements will address high-frequency response limitations, further reduce weight, and integrate Bluetooth functionality to meet modern user expectations. These developments aim to bring the design closer to a true all-in-one headphone solution without compromise.

Declaration of originality

I hereby confirm that this dissertation is my own original work unless referenced clearly to the contrary, and that no portion of the work referred to in the dissertation has been submitted in support of an application for another degree or qualification of this or any other university or other institute of learning.

Intellectual property statement

- i The author of this thesis (including any appendices and/or schedules to this thesis) owns certain copyright or related rights in it (the “Copyright”) and s/he has given The University of Manchester certain rights to use such Copyright, including for administrative purposes.
- ii Copies of this thesis, either in full or in extracts and whether in hard or electronic copy, may be made *only* in accordance with the Copyright, Designs and Patents Act 1988 (as amended) and regulations issued under it or, where appropriate, in accordance with licensing agreements which the University has from time to time. This page must form part of any such copies made.
- iii The ownership of certain Copyright, patents, designs, trademarks and other intellectual property (the “Intellectual Property”) and any reproductions of copyright works in the thesis, for example graphs and tables (“Reproductions”), which may be described in this thesis, may not be owned by the author and may be owned by third parties. Such Intellectual Property and Reproductions cannot and must not be made available for use without the prior written permission of the owner(s) of the relevant Intellectual Property and/or Reproductions.
- iv Further information on the conditions under which disclosure, publication and commercialisation of this thesis, the Copyright and any Intellectual Property and/or Reproductions described in it may take place is available in the University IP Policy (see <http://documents.manchester.ac.uk/DocuInfo.aspx?DocID=24420>), in any relevant Dissertation restriction declarations deposited in the University Library, and The University Library’s regulations (see http://www.library.manchester.ac.uk/about/regulations/_files/Library-regulations.pdf).

1 Introduction

1.1 Background

Headphones have become a ubiquitous device in our lives, with accessibility and usage increasing annually. Each year, more companies introduce new models with enhanced features. Despite rapid innovation, most headphones still rely on the same driver technology introduced over 90 years ago, with its fundamentals remaining largely unchanged [1].

Various driver technologies exist, each with unique characteristics and benefits, yet one drastically dominates public use. This raises the question: Are there alternative technologies that could offer better solutions to the limitations currently accepted?

Consumer headphones typically use a technology called dynamic drivers. While widely adopted due to their cost-effectiveness and simplicity, this type of driver inherently introduces colouration to the audio signal, altering the original sound of the recording [2]. In some cases, such colouration can enhance music enjoyment by adding warmth or punch. However, for professionals or critical listeners, this alteration can be undesirable.

1.2 Motivation

The added colouration can mask subtle details in the sound, making it more difficult to hear the music in the way it was originally recorded. For professionals, this can make it difficult to make accurate decisions during mixing or mastering. For critical listeners, it may prevent full appreciation for the artist's intended expression, losing a sensation that was meant to be felt. While studio headphones can provide more accurate sound, they often sacrifice the versatility of dynamic driver-based designs, which are typically lighter, more compact, and better suited for everyday use. A solution that delivers high-quality sound without compromising on portability could save both time and money, enabling professionals and audio enthusiasts to experience accurate audio from anywhere, with one device.

These concerns served as the motivation for the research presented in this thesis: to investigate whether a novel implementation of an existing technology, specifically planar magnetic drivers with a new magnet configuration, could overcome the limitations of dynamic drivers while retaining the portability and practicality required for everyday use.

Unlike traditional dynamic drivers, which use a cone-shaped diaphragm (a thin material that vibrates to produce sound), this design uses a flat version suspended between magnet arrays, meaning the force is distributed along the entire diaphragm surface, resulting in more accurate and detailed sound reproduction [3]. A Halbach array is a specific magnet arrangement which concentrates the magnetic

field on one side of the magnet array, whilst almost eliminating it on the other side, enabling more efficient usage of magnetic flux [4]. This focused field could also allow for fewer magnets to be used, since less flux is wasted, helping to reduce overall headphone weight, a common limitation of planar magnetic headphones. This planar magnetic configuration with Halbach arrays is represented in Figure 1 :

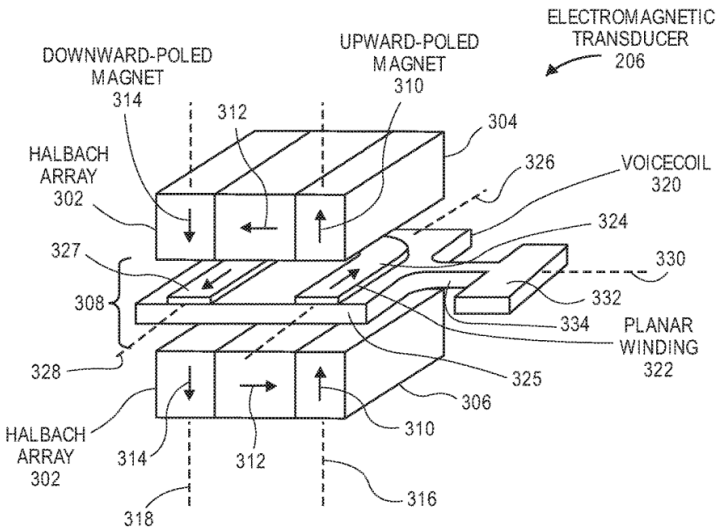


Fig. 1. Apple patent employing planar magnetic driver configuration [5].

To support this investigation, the report will provide a brief overview of the various implementations of driver technologies within headphones, along with their historical context. It will then take a closer look at a technology that is seldom discussed: planar magnetics, and how it differs from more traditional solutions. More specifically, the report will examine whether planar magnetic technology can be leveraged not only to overcome the limitations of other driver types but also to address its own known shortcomings.

1.3 Aims and Objectives

The aim of this report is to explore planar magnetic drivers and investigate a novel approach to their implementation in order to maximise their benefits, such as clear sound quality, while mitigating common compromises like weight and limited portability. This report proposes that planar magnetic drivers offer a competitive, high-performance alternative to other headphone technologies.

To achieve this aim, clear objectives have been defined to limit and focus the scope:

- Find a magnet configuration providing the strongest alternating field at its surface, using simulations to visualise the magnetic field and determine the resulting force on the diaphragm.
- Determine the relative magnetic field distribution on a set of parallel current-carrying traces by creating simulations based on physical principles.

- Select a suitable diaphragm material by considering mechanical properties such as stiffness, mass, and flexibility, along with availability and ease of manufacturing.
- Design a PCB with a serpentine trace layout, ensuring that the area of highest magnetic flux density overlaps with the magnetic field loops created by the magnets.
- Design and 3D print a driver enclosure to house the selected magnet configuration and hold the PCB in tension.
- Produce and analyse frequency response plots of the headphones, alongside those of a commercially available model, to evaluate relative performance and viability as an alternative.

1.4 Report Structure

This report commences with a literature review, providing a brief overview of alternative technologies. This is followed by the methodology, which outlines the theoretical development of the project and presents the idealised plan to be followed during implementation. The implementation section then demonstrates this plan in practice, selecting variables based on real-world constraints or the absence thereof. Testing follows, where the performance of the headphones is evaluated and visualised. The discussion section then uses mathematical logic to analyse the results in order to build a deeper understanding of the driver's behaviour. Finally, the conclusion summarises key insights and suggests potential improvements for future research.

2 Literature Review

2.1 Types of driver technology

Although various driver technologies have emerged over time, they all rely on the same fundamental principle established in the 1920s: electrical energy is converted into mechanical wave energy by applying force to a diaphragm, which vibrates to move air and produce sound [2]. Most advancements since then have focused on improving materials, magnet strength, and acoustic tuning through ear cup design [1]. To understand their evolution, it is important to examine the historical timeline of these technologies.

2.1.1 Dynamic drivers

Dynamic drivers are the most common type of headphone driver, with the core technology developed in the 1920s [6] and becoming commercially significant between the 1930s and 1940s [7]. Their continued utilisation is due to their simplicity and cost-effectiveness. A dynamic driver consists of a

coil attached to a diaphragm, usually cone-shaped, suspended within a magnetic field. When electric current flows through the coil, it creates a magnetic field that interacts with the static field of the magnet, causing the diaphragm to move and produce sound [8].

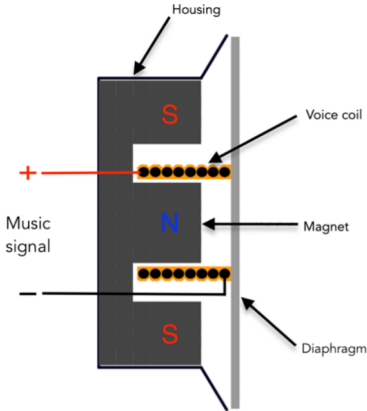


Fig. 2. Internal structure of a dynamic driver, illustrating the voice coil, diaphragm, and magnet arrangement [8].

This driver configuration provides a large diaphragm for movement, allowing it to displace large amounts of air, increasing perceived loudness. The shortcoming of this technology is visible in Figure 2: The coil is located at the centre of the diaphragm surface, and since this is the inducer of force applied, the diaphragm does not experience a uniform force across its surface, which can lead to distortion and uneven movement, affecting the accuracy of sound reproduction [2]. This non-uniform distribution of force can cause certain areas of the diaphragm to move more or less than others, leading to issues such as frequency response anomalies or sound colouration. This issue is less prominent in alternative headphone drivers, which apply force evenly across the entire diaphragm surface, such as planar magnetic or electrostatic drivers [8].

Each implementation has its trade-offs. Dynamic drivers are advantageous due to their large cone, which displaces a lot of air and produces greater loudness. However, a larger cone also has more mass, increasing its inertia and making it harder to stop the diaphragm once in motion. This can result in a less accurate representation of the original sound signal and may introduce resonance peaks. Designing drivers involves balancing several conflicting goals, and a successful implementation requires carefully chosen trade-offs [1].

2.1.2 Electrostatic Drivers

In an attempt to mitigate the limitations of the dynamic drivers, a new type of driver technology called electrostatic drivers was introduced during the 1950s [9]. The primary goal was to eliminate the distortion created by the mechanical limitations of dynamic drivers by applying an even and uniform force across the diaphragm's surface.

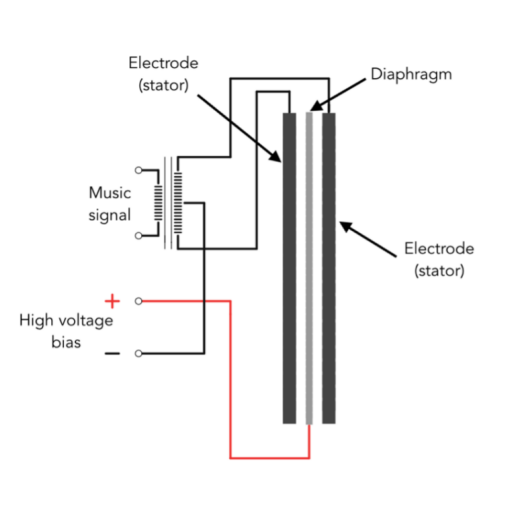


Fig. 3. Internal structure of an electrostatic driver, showing a thin diaphragm suspended between two charged plates and driven by a high-voltage bias and audio signal [8].

In this driver configuration, there are no magnets to drive the diaphragm, nor is the diaphragm cone-shaped. Instead, the diaphragm is made of a very thin, flexible film-like material. This diaphragm is electrically charged and is suspended between two electrically charged metal plates. The polarity of charge on the metal plates corresponds to the alternating "music signal" from the amplifier, meaning that the plates will have opposite charges at any given moment [1].

The diaphragm moves due to electrostatic forces, similarly to how a balloon sticks to a wall after being rubbed against your head. When rubbed, the balloon becomes negatively charged, and when brought near a neutral wall, its electrons are repelled and protons are attracted, causing the balloon to stick. In this case, the diaphragm represents the balloon, and the metal plates are the wall. The diaphragm is positively charged and is attracted to the negatively charged plate and repelled from the positively charged one. As the audio signal alternates the charge on the plates, the diaphragm is alternately attracted to one plate and repelled by the other, causing it to move back and forth, generating sound.

This design eliminates a key limitation of dynamic drivers: mass and inertia. The lightweight diaphragm allows for more precise control over its movement, resulting in an improved transient response. This leads to a highly detailed representation of the input signal, high clarity, and little distortion. As reiterated there are always drawbacks; in this case, the electrostatic drivers act as large capacitors. The issue is that the impedance of capacitors is not constant across all frequencies, this type of behaviour is known as a reactive load [1]. Therefore, at certain frequencies, the amplifier sees the load as a near short circuit due to the very low impedance, which can result in substantial current flow and potentially stress the amplifier. To solve this, a buffer would be needed between the amplifier and load, matching the impedance of the amplifier to the impedance of the drivers. A transformer can accommodate such demands, ensuring that the amplifier perceives the correct load and helps convert the low-voltage signal from the amplifier into the high-voltage signal needed for the

electrostatic panel. The challenge, however, is that designing a transformer capable of handling high power across the full frequency range is complex and costly [9].

2.1.3 Planar magnetic drivers

As demonstrated, there are numerous complications when attempting to strike a balance between the detailed sound reproduction of electrostatic drivers and the accessibility of dynamic drivers. Planar magnetic drivers were invented in the 1970s in an attempt to combine the best features of both technologies, bridging the gap between clear sound quality and practicality [10]. The mechanical characteristics of planar magnetic headphones are similar to those of electrostatic drivers, using a thin diaphragm, but this time suspended between an array of magnets. This design provided the high sound quality facilitated by electrostatic drivers whilst rapid advancements in magnet technology during the 2000s made them increasingly accessible [8].

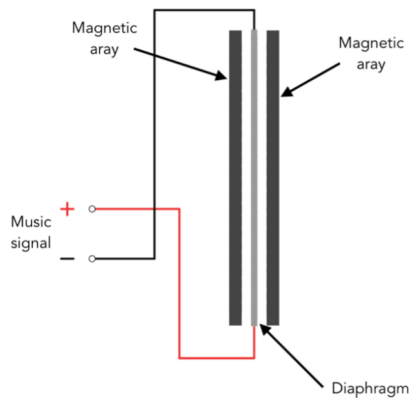


Fig. 4. Internal structure of a planar magnetic driver, illustrating a pair of magnetic arrays with a diaphragm suspended between [8].

Similar to electrostatic drivers, a thin diaphragm is used to displace air, but instead of a fixed charge, it has a serpentine-wound coil that carries an alternating audio signal as a current. The diaphragm is suspended between two magnet arrays, configured so their fields superpose. The traces on the diaphragm align with the magnetic field created by the magnets, so when current flows through them, their induced field interacts with the magnets, creating a uniform force across the surface of the diaphragm. This implementation eliminates the heavy diaphragm and the non-uniform force seen in dynamic drivers, resulting in a more detailed and less distorted sound [8].

Planar magnetic drivers also resolve the issues faced by electrostatic drivers, as the load is purely resistive and remains constant across all frequencies, making them easier for the amplifier to drive and eliminating the need for a high-voltage source or transformer [1]. However, the primary drawback is that planar magnetic headphones tend to be heavier due to their integration of magnets, for this

reasoning they are not typically used outside of sedentary listening. Over the years, advancements in magnet technology have contributed to the development of lighter and more efficient magnetic structures, improving portability and comfort. Despite these improvements, the perception of planar magnetic headphones is that there is a clear trade-off between comfort and versatility for sound quality [10].

However, as specified in the introduction, this report explores the use of a Halbach array as a solution to this problem. Interestingly, during the development of the product, it was discovered that Apple had patented a similar concept in 2015 [5], employing a comparable magnet configuration using paired Halbach arrays. This configuration has each adjacent magnet rotated 90° relative to previous:

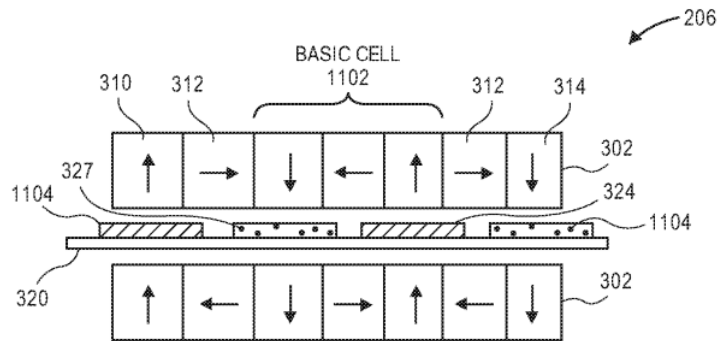


Fig. 5. Apple patent employing Halbach magnet Configuration [5].

This application offers similar advantages to traditional planar magnetic drivers, but with a key enhancement: the Halbach array configuration directs most of the magnetic flux across the gap where the coil sits, while cancelling it on the opposite side. This efficient use of magnetic flux results in a stronger Lorentz force acting on the diaphragm [5]. As a result, fewer magnets are needed to achieve the same performance, enabling a lighter and more compact form factor.

The independent convergence of such ideas underscores the relevance and feasibility of this design approach, and is a major reinforcement of the underlying concept. However, while Apple's patent outlined the theoretical potential of such a configuration, it stopped short of demonstrating whether the approach could deliver on its promises in practice. This project takes that concept further, by fully implementing, testing, and evaluating the design, to determine whether this technology is viable for high-fidelity, portable audio applications. Building on this, the following section will delve into the theoretical development of the proposed implementation, outlining its core principles.

3 Methodology

3.1 Theoretical Development

Sound is caused by the displacement of air molecules due to vibrations. These molecules do not travel with the sound wave; instead, they move back and forth in place parallel to the direction of the wave's propagation. As they do this, they either compress together (compression) or spread apart (rarefaction). This cycle of compression and rarefaction moves through the air as a pressure wave, carrying energy from the source to your ears, where it is interpreted as sound. The difference between the highest and lowest pressure points in a wave is called its amplitude, and the greater the amplitude, the louder the perceived sound [11].

Accordingly, to create sound, air molecules must be displaced through vibrations. In headphones, this is achieved using a diaphragm. A diaphragm is a material that vibrates in response to a force. The diaphragm's motion determines the sound perceived by the ear and is directly influenced by the force acting upon it. Therefore, the accuracy of the perceived sound depends on how precisely an input sound signal is converted into force, which then drives the diaphragm's motion.

For the diaphragm to create compressions and rarefactions, it must receive a push-pull force. In planar magnetic headphones, this force comes from an interaction of magnetic fields. A static magnetic field is generated by suspending the diaphragm between two arrays of magnets. However, a static magnetic field alone isn't enough. The diaphragm needs a changing force to vibrate and produce sound. This changing force comes from an alternating magnetic field, which is produced by conductive traces on the diaphragm carrying an alternating current (AC). When the AC current flows through these traces, it generates an alternating magnetic field around them, which interacts with the static field from the permanent magnets.

This interaction produces an alternating force on the diaphragm, causing it to move back and forth. The strength of this force on any given trace is determined by Lorentz Force Law:

$$F = I \cdot B \cdot L \quad (1)$$

Where F is the force felt by the trace, I is the current through the traces, L is its effective length, and B is the magnetic flux density of the static magnetic field. The total force on the diaphragm in planar magnetic headphones is the sum of the forces on all the individual traces. Since each trace carries current and interacts with the static magnetic field from the permanent magnets, the total force can be derived as follows:

$$F_{total} = N \cdot I \cdot B \cdot L \quad (2)$$

Where variables have their aforementioned meaning, F_{total} is the total force felt by the diaphragm and N is the number of traces subjected to the force.

Understanding how the diaphragm responds to this force is essential for predicting the frequency response and resonance behaviour of the system. Since the external force acting on the diaphragm is defined, an equation of motion can be derived to describe its response. The calculations are simplified by the absence of free vibrations during normal operation of planar magnetic drivers, allowing the system to be modelled as a second-order mass-spring-damper system.

$$F_{total}(t) = M\ddot{x} + c\dot{x} + Kx \quad (3)$$

Where F_{total} maintains the previous meaning, $M\ddot{x}$ is the inertial force, $c\dot{x}$ is the damping force, and finally Kx is the restoring force, which represents the restoring tension in the diaphragm. This can be further analysed to find the effects of the force on the system within the frequency domain, by simplifying the differential equation of motion using the Laplace transform:

$$\mathcal{L}\{F_{total}(t)\} = \mathcal{L}\{M\ddot{x} + c\dot{x} + Kx\} \quad (4)$$

$$F_{total}(s) = M(s^2 X(s)) + C(sX(s)) + KX(s) \quad (5)$$

$$F_{total}(s) = X(s)(Ms^2 + Cs + K) \quad (6)$$

The equation can be rearranged to get a transfer function for the frequency response of the system:

$$H(s) = \frac{X_s}{F_{total}(s)} = \frac{1}{Ms^2 + Cs + K} \quad (7)$$

$$H(s) = \frac{1}{Ms^2 + \frac{C}{M}s + \frac{K}{M}} \quad (8)$$

$$H(s) = \frac{1}{Ms^2 + 2\zeta\omega_n s + \omega_n^2} \quad (9)$$

Where ζ is the damping ratio and ω_n is the natural frequency of the system.

This transfer function describes the frequency response of the diaphragm, demonstrating how it reacts to external forces across different frequencies. It highlights the influence of mass M , damping C , and stiffness K on the system's behavior, each characteristic of the system essentially depends on these

these three variables, so it is vital to see the relationships that they hold. Firstly, the natural frequency (ω_n):

$$\omega_n = \sqrt{\frac{K}{M}} \quad (10)$$

Knowing the relationship of the natural frequency of the system is paramount to avoiding resonance peaks in the frequency response. Ideally, the system's natural frequency would lie outside the audible frequency range to prevent resonances, which occur when the excitation frequencies approach the natural frequency of the material. However, due to the distributed and tightly controlled nature of planar magnetic diaphragms, in comparison to single-point dynamic drivers, planar drivers are inherently less prone to sharp resonance peaks, making their response more linear and predictable across the frequency spectrum.

Secondly, the damping ratio (ζ):

$$\zeta = \frac{C}{2\sqrt{MK}} \quad (11)$$

The damping ratio determines how quickly oscillations dissipate after the diaphragm is subjected to an external force, thereby controlling the system's transient response. Ideally, a higher damping ratio is preferred, as it reduces unwanted resonances and helps the diaphragm settle quickly. Achieving this typically requires a low diaphragm mass while also minimising stiffness to maintain responsive movement.

Finally, the gain of the system:

$$\text{Gain} = \frac{1}{M} \quad (12)$$

The gain relationship clearly indicates the mass of the diaphragm is inversely proportional to the system's responsiveness, meaning a lighter diaphragm more efficiently converts the input force into motion.

The conclusion drawn from these relationships is that a light mass and low stiffness diaphragm is ideal for an efficient headphone driver.

Fundamentally, the operation of the drivers can be described using a combination of Equation (2), which represents the external force applied to the diaphragm, and Equation (9), which describes the diaphragm's response to that force in the frequency domain. Equation (2) highlights how the force is influenced by the magnetic flux density, current, and number of traces, demonstrating that increasing

any of these variables increases the total force applied to the diaphragm. Meanwhile, Equation (9) outlines how the system's behaviour is governed by mass, damping, and stiffness.

These relationships provide insights into how changes in diaphragm material and geometry affect natural frequency, damping ratio, and overall gain. Together, these two equations form the theoretical foundation for key design decisions throughout the project.

3.2 PCB Optimisation

Building on the understanding of how diaphragm mass, stiffness, and damping influence system response, this knowledge informs the design of the printed circuit board (PCB). While selecting a lightweight and flexible diaphragm material is essential, additional factors must be considered to optimise performance. Specifically, the electrical resistance of the diaphragm traces and the alignment of the static and alternating magnetic fields play a critical role in ensuring efficient force generation and accurate control of diaphragm motion.

This section outlines the theoretical considerations and design process for PCB optimisation, covering:

- **PCB Trace Layout** – Optimising trace width and length to increase total resistance of the diaphragm.
- **Diaphragm Material Selection** – Choosing a lightweight, flexible material that maintains uniform tension while ensuring durability.
- **Magnetic Field Alignment** – Simulating both static and alternating magnetic fields to determine their optimal relative positioning.

Starting with the PCB trace layout, it is important to consider its effect on resistance, and in turn, the effect that resistance has on the system.

The impedance of the diaphragm influences not only the system's efficiency and the current drawn from the amplifier, but also the damping factor of the headphones. The damping factor, defined as the ratio of load impedance (headphones) to source impedance (amplifier), measures how effectively the amplifier can control the diaphragm's motion once a signal has stopped [12]:

$$DF = \frac{Z_{\text{load}}}{Z_{\text{source}}} \quad (13)$$

Where DF is the damping factor, Z_{load} is the impedance of the diaphragm and Z_{source} is the impedance of the amplifier. Planar magnetic drivers have a purely resistive load; therefore, their impedance

curve is virtually flat, this means a constant current and voltage can be drawn for all frequencies, making it a simple load for an amplifier to drive [1]. Thus, in comparison to a driver type like dynamic drivers, where there is significant impedance variation across frequencies, damping factor is less essential. Nonetheless, since the frequency response plot of the drivers will not be perfectly flat and may experience sudden changes in impedance, the damping factor still plays a useful role in controlling transient responses, a behaviour that will be revisited in the experimental results section.

The method for increasing the impedance of the load is twofold: reducing the width of the current-carrying trace, and increasing its length. Using the minimum allowable width and the maximum feasible length maximises resistance, as described by:

$$R = \rho \cdot \frac{l}{w \cdot t} \quad (14)$$

Where R is the resistance, ρ is the resistivity, l is the length, w is the width, and t is the thickness of the trace. Reducing the trace width increases resistance directly and also enables more traces to be routed within the same area. In turn, this extends the total trace length, further increasing the overall resistance of the diaphragm.

Tracks are parallel sets of traces on a PCB. The relative shape of a track's magnetic field distribution depends on the configuration of the traces within it. These traces are typically parallel, with a separation distance defined by manufacturing constraints. With this configuration established, the magnetic field distribution can be derived by first calculating the magnetic flux density B of an individual current carrying trace, which can be defined using Ampere's law:

$$B = \frac{\mu_0 I}{2\pi r} \quad (15)$$

Where B is the magnetic flux density, μ_0 is the permeability of free space, I is the current through the trace, and r is the radial distance from the trace. Since the focus is primarily on the relative field distribution, the magnitude of the current, I , and the number of traces in a track can be disregarded for this analysis. To find the flux density at any given point due to multiple traces, the principle of superposition is applied. This means the total magnetic field at any point is the vector sum of the individual magnetic fields at that point. This can be visualised using a Python script to plot the field distribution for an arbitrary number of traces per track. The code for this analysis is provided in Appendix A.7.

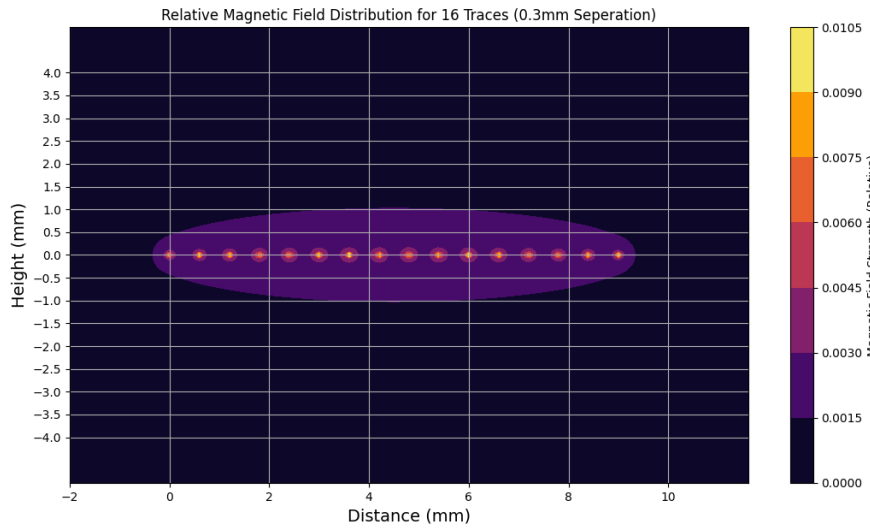
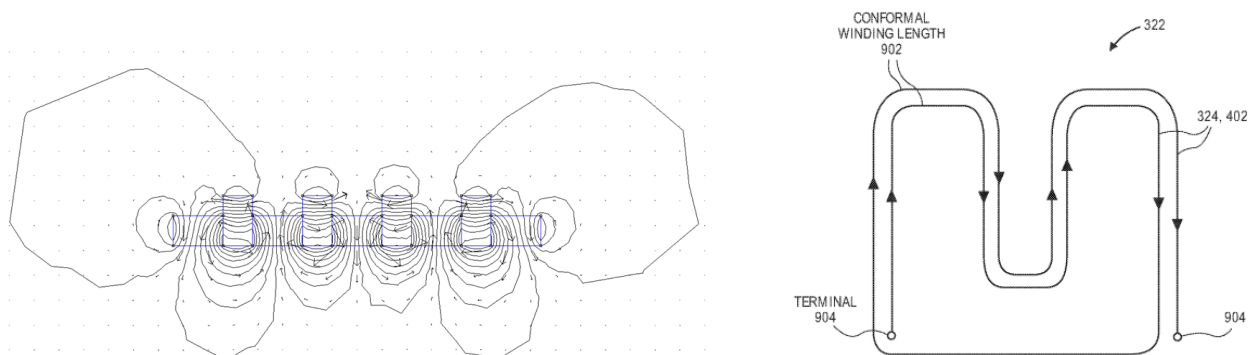


Fig. 6. Relative Magnetic Field Distribution For a Track.

Figure 6 demonstrates the relative magnetic field distribution for a track. The track contains traces, each carrying current and producing a magnetic field. The total field distribution is symmetrical about the centre of the track, as expected due to the symmetrical arrangement of the traces within it. The centre exhibits the greatest summation of vector magnetic fields. Therefore, to maximise efficiency in the drivers, the centre of the track should align with the regions of highest magnetic flux density induced by the magnetic array.

Whilst the optimal track positioning relative to the static magnetic field has been established, the exact configuration of tracks on the PCB must still be defined. The diaphragm is suspended in a spatially alternating magnetic field, where the field direction reverses from magnet to magnet, as shown in Figure 7a. To interact effectively with this pattern, the current in the PCB traces must also alternate. This is achieved through a serpentine layout, where the current reverses at each fold. As a result, all traces within a single track carry current in one direction, while adjacent tracks carry it in the opposite direction, as illustrated in Figure 7b.



(a) Spatially alternating static magnetic field, simulated using FEMM.

(b) Example of serpentine trace layout, as illustrated in Apple's planar magnetic patent [5].

Fig. 7. Magnetic field and trace layout shown in relation to each other.

This alignment ensures that the magnetic fields generated by the traces constructively interact with the spatially alternating static field, producing a uniform and balanced force across the diaphragm. The serpentine shape implemented on the PCB is visualised using a Python script (Appendix A.7) and shown in Figure 8. The exact layout dimensions will be refined once the magnetic field loop width and magnet size are determined in Section 4.1, as these parameters will inform the track width.

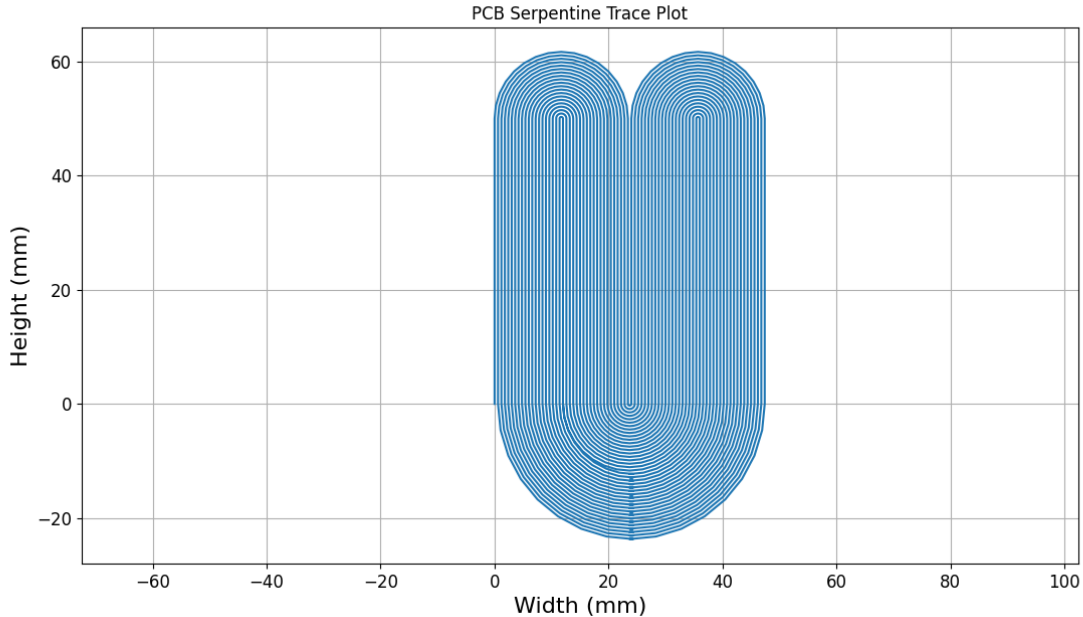


Fig. 8. Simulated serpentine trace layout generated using Python for preliminary PCB routing visualisation.

Figure 8 shows the theoretical design of the PCB, with an arbitrary number of traces per track. The exact number of traces per track is determined based on the magnetic field loop width created by the magnets. Since the audible frequency range only extends up to 20 kHz, high-frequency considerations like crosstalk and electromagnetic interference are minimal. Consequently, traces can be routed close together without significant risk of noise. However, standard design practices still apply. In particular, bends in traces should be rounded rather than sharp, avoiding trace width variation along the bend, which could cause impedance changes and result in signal reflections.

The next step involves selecting a suitable substrate material for the PCB. Given the application's requirement for flexibility and minimal inertia, as justified in Section 3.1, a polyimide-based flexible circuit is the optimal choice. Polyimide offers both flexibility and low mass, making it ideal for supporting the diaphragm's dynamic response. Additionally, polyimide-based PCBs possess high tensile strength, which makes them resistant to warping [13]. This resistance is essential for consistent sound reproduction, as it mitigates the risk of resonance peaks occurring at varying locations.

The flexibility and low mass of polyimide ensure the diaphragm responds sensitively to input signals, maximising system gain, as described by Equation (12). Using a low-mass substrate also affects the

damping factor, as shown in Equation (11). A higher damping factor gives the amplifier greater control over diaphragm movement, allowing oscillations to dissipate more quickly after input changes. This control is critical for accurately reproducing transients and maintaining stability.

3.3 Permanent magnet array optimisation

The sound quality of planar magnetic drivers is heavily influenced by the magnet configuration, as it directly determines the force acting on the diaphragm. A stronger force enables tighter control over the diaphragm's motion, reducing distortion by allowing it to start and stop more precisely in response to the input signal. From Equation (2):

$$F_{total} = N \cdot I \cdot B \cdot L \quad (2)$$

It is evident that for a given force F , increasing the magnetic flux density B allows the required current I to be reduced, assuming the conductor length L remains constant. Moreover, since the diaphragm behaves as a purely resistive load with relatively constant resistance, the electrical power required is directly proportional to the square of the current.

$$P = I^2 \cdot R \quad (16)$$

Hence, by increasing B , the system requires less current I for a given force F , which in turn reduces power consumption P .

A Halbach array is the ideal magnet configuration to meet this criterion, as it maximises the magnetic flux density (B field) on the side facing the diaphragm, providing a strong and focused magnetic field. This is useful as the magnetic flux density that would normally be wasted in air is redirected towards the diaphragm, increasing efficiency and reducing electromagnetic interference with surrounding technologies. As mentioned, this increased B reduces power required.

By concentrating more magnetic flux toward the diaphragm, fewer magnets are needed to achieve the same force, as the flux is used more efficiently than in configurations with unfocused or stray fields. This results in a reduction in overall system weight, directly addressing a key limitation of traditional planar magnetic designs. Utilising a Halbach array improves efficiency, reduces weight, and ultimately enhances both performance and comfort, making the technology more versatile.

To further optimise performance, the choice of magnet material is also critical. A magnet with high magnetisation directly increases the magnetic flux density B , which, as discussed, improves overall system efficiency. Additionally, using lightweight magnetic materials helps reduce the total mass of the system, supporting the goal of weight minimisation in planar magnetic driver designs.

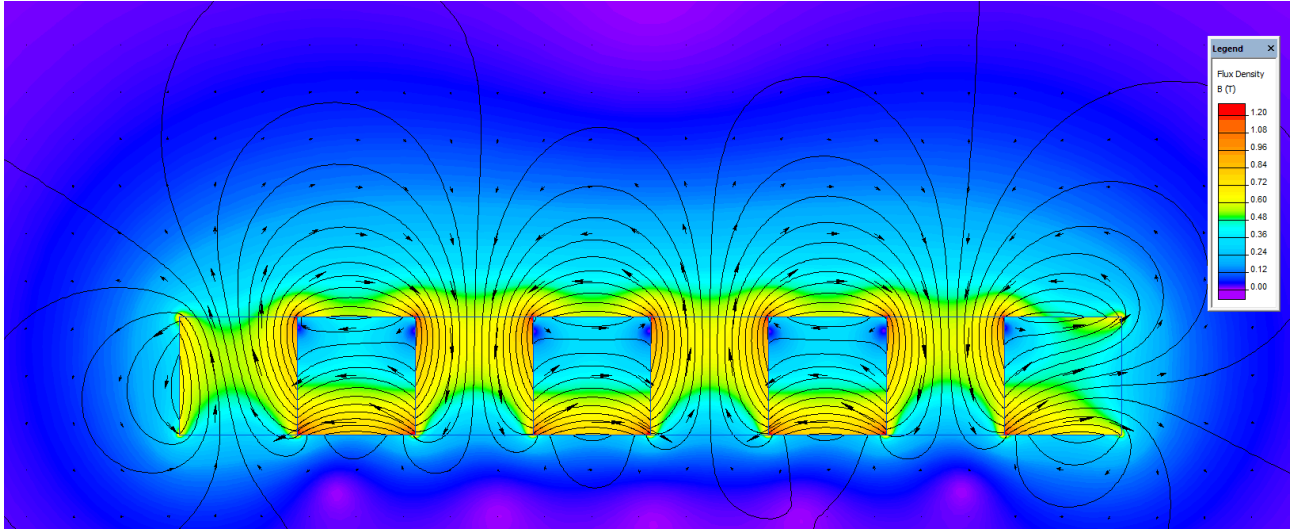


Fig. 9. Spatially alternating magnetic field of Halbach array [22].

Figure 9 shows the magnetic field distribution of a Halbach array, with a strong localised field on the top, represented by the higher density of magnetic field lines. The vector arrows indicate the direction of the magnetic field at each point, illustrating how the field alternates spatially along the length of the array. This means the direction of the field loops reverses from one magnet to the next.

In the final implementation, two such arrays will be used, with their fields superposing and a flexible PCB suspended between them.

4 Design and Implementation

This section focuses on translating the theoretical optimisations defined in section 3.1, into a physical, manufacturable design, taking into account real-world constraints such as component availability and assembly limitations. In this section the variables of the system will be chosen and justified.

4.1 Permanent Magnet Design

In magnetic applications, there are two main categories of magnets: electromagnets, which require an electric current to generate an electric field, like the copper traces on the diaphragm, and permanent magnets, which maintain their magnetism without external power. There are several types of permanent magnets each with their own characteristics, ranging from Neodymium, Alnico, Ceramic and Samarium Cobalt. When selecting the type of magnet, it must meet criteria defined in Section 3.3: have a strong magnetisation and a light form factor.

Table 1. Magnetic material properties [14].

Magnetic material	Density (g/cm ³)	Max Energy product BH_{max} (MGOe)	Coercive Force Hc (Oersteds)	Maximum Operating Temperature (°C)	Curie Temperature (°C)
Neodymium 35	7.4	33-36	≥ 10900	80	312
Ceramic 8	4.9	3.5	≥ 3200	204	450
SmCo 30	8.4	28-30	≥ 9900	350	820
Alnico 8 (sintered)	7	4	≥ 1500	450	860

The most relevant property of this table is the maximum energy product (BH_{MAX}), which is a measure of the magnetic energy a material can store per unit volume. Neodymium has the highest BH_{MAX} , meaning it produces the strongest magnetic field per unit size, which is ideal for this compact use case within headphones. In addition, neodymium has the largest coercivity, which measures the ability of the material to withstand an opposing magnetic field before becoming demagnetized, an important property since the permanent magnets will be subjected to the magnetic field produced around each of the traces. Finally, characteristics such as maximum operating and Curie temperature are sufficient for the use case, since the headphones will not reach such high temperatures.

The permanent magnets chosen for use in the drivers are N35-grade neodymium magnets. These were selected for three key reasons. Firstly, they are significantly stronger than other magnets, with an adhesion force 5–6 times greater than that of ceramic magnetic materials, providing a large magnetic flux density B [15]. Secondly, neodymium magnets have the highest maximum energy product of any material listed in Table 1, meaning they can store more magnetic energy per unit volume. Combined with their relatively low density of 7.4 g/cm³, this makes them ideal for generating strong magnetic fields in a compact, lightweight form factor. Finally, neodymium magnets provide greater energy potential per unit volume than any other magnet type [16].

Yet, there are important considerations when working with neodymium magnets. Whilst they are magnetically strong, they are also extremely brittle and must be handled with care. If allowed to snap together due to magnetic attraction, they can easily chip or fracture. The main challenge lies in the initial arrangement of the magnets. However, since the Halbach array is an inherently stable structure, once the magnets are properly aligned, they are less likely to shift or jump out of place.

The selected magnet size of 50 mm × 5 mm × 3 mm was chosen based on a balance between availability and the physical constraints of the headphone assembly. While larger magnets can provide greater force, this design is constrained to a compact area, and minimising weight is a key consideration. This particular size is readily available on the market, which is especially important given the limited project time frame. Additionally, the dimensions fall within the typical size threshold for headphone ear cup designs, making them well-suited for integration.

To evaluate the performance of the selected neodymium magnets, they were arranged in a two-row Halbach array and simulated using FEMM. This allowed for direct visualisation of the magnetic field distribution resulting from the chosen configuration. The ability of the Halbach structure to concentrate flux on one side and cancel it on the other, as previously discussed in Section 3.3, is now clearly visible. Figure 10 illustrates this, highlighting the spatial variation and confinement of the magnetic field, with low flux density shown at the top. This behaviour is key to ensuring efficient force transfer to the diaphragm while minimising losses.

Given that a typical headphone earcup has an inner width of approximately 50 mm, using 5 mm wide magnets allows for up to 10 magnets across the width. However, to maintain symmetry around the centre of the array, 9 magnets were used, as displayed below:

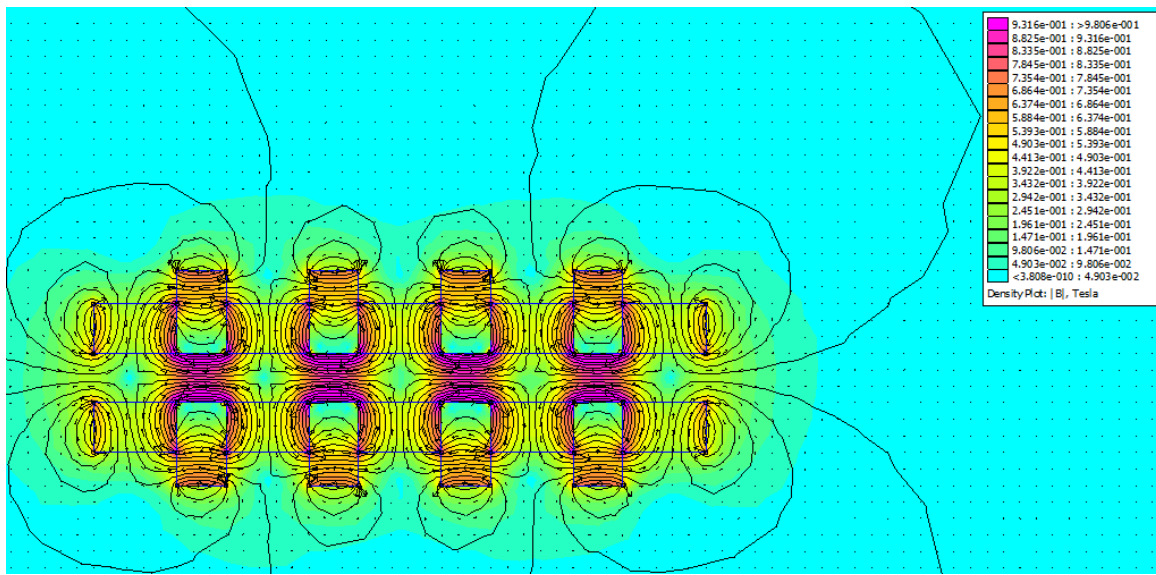


Fig. 10. Flux density plot of 2 row, 0 mm gap Halbach array.

Figure 10 displays the magnetic flux density as a colour density plot, in which darker regions represent areas of higher magnetic flux density B . From this plot, it is evident that there are four distinct magnetic loops, with high flux density concentrated near their surfaces, reaching a peak value of 0.93T.

To better understand how these fields influence diaphragm motion, a tangential flux density plot at the midpoint of the air gap can be derived. The tangential plot in Figure 11 reveals the variation in flux density along the length of the diaphragm, representing the magnetic field profile that the current-carrying traces will interact with.

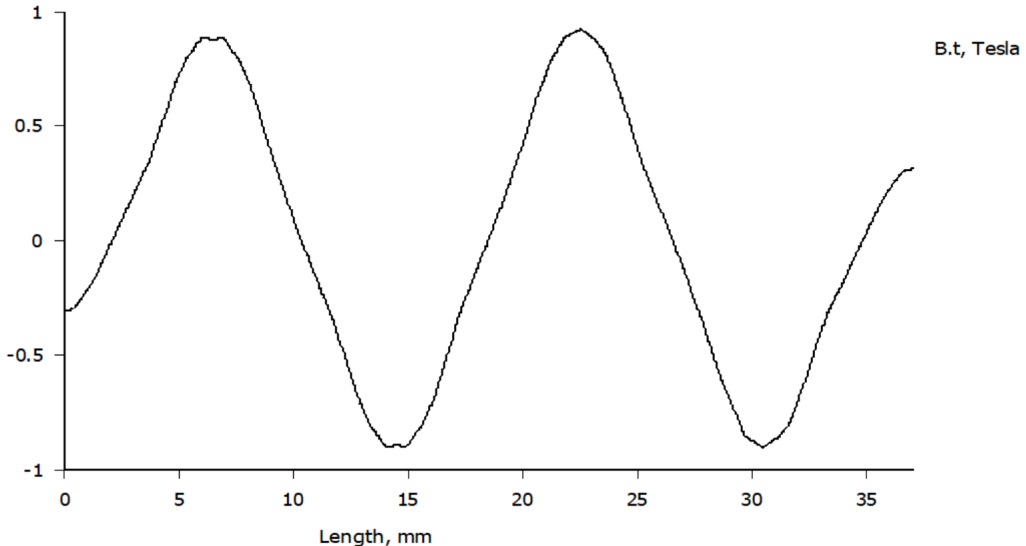


Fig. 11. Tangential flux density plot of 0 mm gap, 2 row Halbach array.

Figure 11 allows us to clearly visualise the spatial variation in magnetic flux density across the diaphragm, alternating in direction between approximately $\pm 0.9 B_t$.

Since the magnets are placed directly in contact, this configuration produces the strongest magnetic field at the surface. However, this comes at the expense of narrower magnetic field loops, which in this case measure approximately 8 mm in width.

This has important design implications. A larger loop width is generally preferable, as it allows more traces to be placed within each magnetic loop, which increases the total resistance of the load. More importantly, it increases the number of current-carrying segments interacting with the magnetic field, leading to a more evenly distributed force across the diaphragm. This improves the responsiveness of the diaphragms motion, contributing to better sound reproduction.

At The University of Manchester, PCB design constraints specify a minimum trace width and separation of 0.3 mm each. Based on this, an equation can be derived to estimate the number of traces n that can fit within a single magnetic field loop:

$$\text{Magnetic field loop width} = 0.6n - 0.3 \quad (17)$$

$$8 = 0.6n - 0.3 \quad (18)$$

$$n = \frac{8.3}{0.6} = 13.83 \quad (19)$$

From Equation (17), it is evident that in this configuration, only 13 traces can fit within a single magnetic field loop. With the number of traces established and the PCB design defined in Section 3.2, the

total resistance of the layout can be calculated using the Python script provided in Appendix A.7. The resulting load resistance is approximately 14.1Ω . To increase this resistance, the width of the magnetic field loop would need to be increased, allowing more traces per track, which in turn requires greater separation between magnets. Increasing the number of traces provides two key benefits: firstly, it raises the load resistance, thereby increasing the damping factor; secondly, it results in a more even distribution of current and force across the PCB.

To explore this, a revised configuration was modelled with 2 mm spacing between each magnet. This separation allows for wider magnetic field loops. The 2 mm gap was chosen based on the minimum printable resolution of the 3D-printed enclosure, defined by the constraints at The University of Manchester. Another FEMM simulation was conducted to visualise the resulting magnetic field profile for this revised configuration. The aim was to assess whether the increased field loop width would enable a more efficient serpentine trace layout without severely compromising magnetic performance.

The outcome of this simulation is shown in Figure 12:

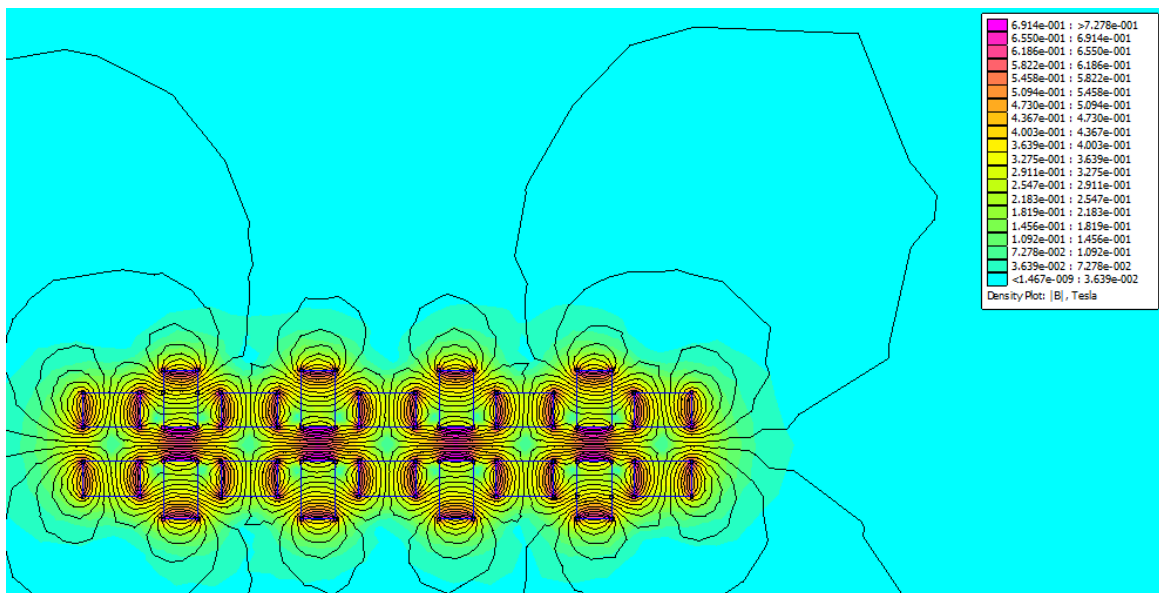


Fig. 12. Flux density plot of 2 row, 2 mm gap Halbach array.

Figure 12 shows a slightly different configuration, incorporating a gap between the magnets to increase the width of the individual field loops. This setup produces a magnetic field loop with a width of 12 mm. Using Equation (17), this setup allows for a maximum of 20 traces per track, which is seven more traces per track than the previous configuration. With four tracks needed in total, one for each loop, this results in an additional 28 lengths of the 50 mm traces. According to the revised resistance calculation (code in Appendix A.7) , this layout results in a load resistance of approximately 22.98Ω , representing a significant increase of 8.9Ω from the previous PCB configuration.

Additionally, this figure clearly depicts that the area of highest magnetic flux density is concentrated at the centre of each loop. This aligns with the findings in section 3.2, where the magnetic field

distribution was shown to peak at the centre and be symmetrically distributed around the tracks. Therefore, the tracks should be positioned directly beneath or above the centre of each magnetic loop to maximise force interaction and ensure consistent performance. The tangential field can be visualised for this configuration:

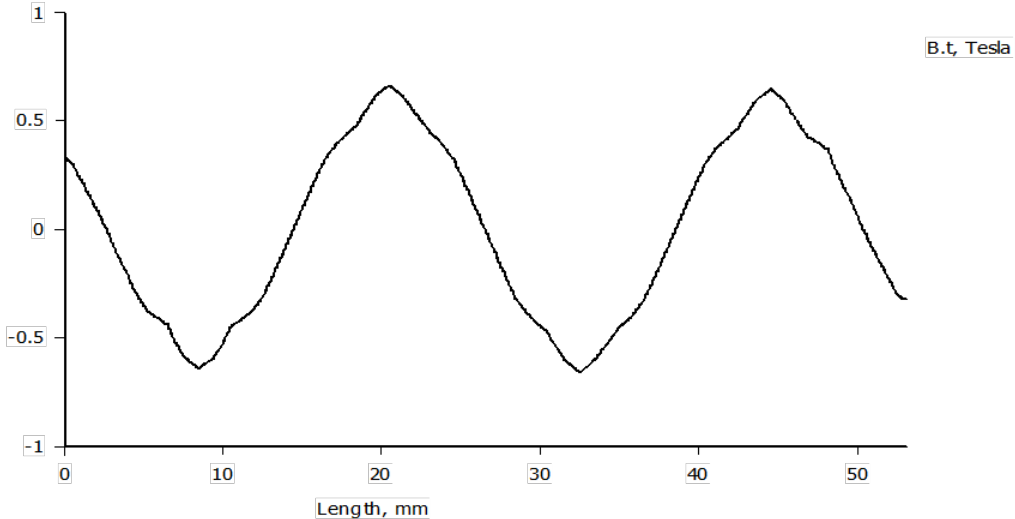


Fig. 13. Tangential flux density plot of 2 mm gap, 2 row Halbach array.

Figure 13 confirms that the 2 mm gap configuration maintains distinct field peaks at approximately $\pm 0.9 B\hat{t}$, supporting precise force application across the diaphragm.

To conclude, the 2 mm gap configuration was chosen because it allows for a greater number of traces per track, leading to a more even current distribution, and a larger resistance load. This results in a uniform force across the diaphragm, reducing distortion and improving sound clarity. Additionally, the wider magnetic field loops align well with the traces, ensuring consistent diaphragm movement. The slight reduction in flux density is a worthwhile trade-off for better accuracy and detail in sound reproduction.

Since the configuration has been established, it must now be implemented. To create a Halbach array, the poles of the magnets are arranged in a periodic pattern such that the direction of the magnetic field rotates around the array. This arrangement is shown in the figure below:

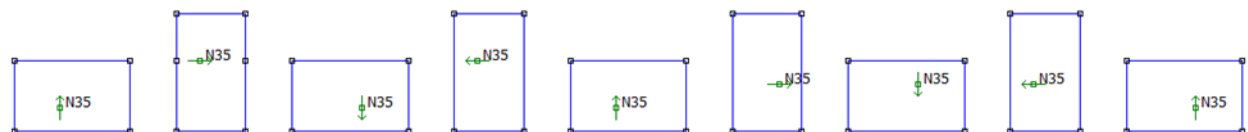
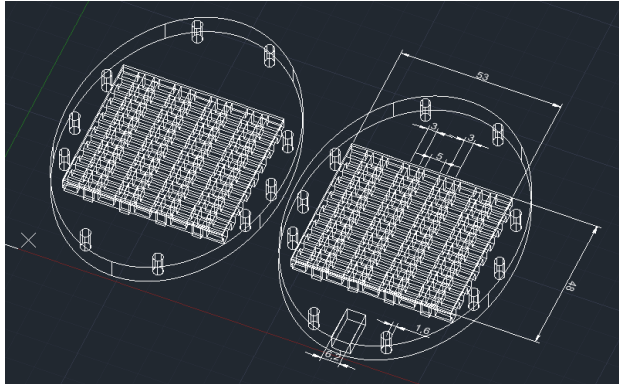


Fig. 14. Halbach array orientation.

Figure 14 displays the final magnet configuration. A total of 9 magnets were used, generating 4 circulating flux paths, similar to those shown in Figure 12.

To maintain proper alignment and spacing of the magnets, a 3D-printed enclosure will be designed, featuring alternating slots: 3 mm deep by 5 mm wide, and 5 mm deep by 3 mm wide. These slots will securely hold the magnets in their intended orientations, with a fixed 2 mm gap between them.



(a) CAD design of driver enclosure with magnet slots.



(b) Assembled enclosure with Halbach magnet array.

Fig. 15. Driver enclosure from CAD design to assembled magnetic structure.

Figure 15a displays the driver enclosures with the alternating slots for the magnets. When designing the shape of the enclosure, it was known a minimum height of 50 mm would be required to accommodate the magnet array, along with additional space to support the serpentine trace layout.

The total width of the magnet array is determined by the sum of the widths of the magnets and the gaps between them, as shown:

$$\text{Minimum width} = 5 \times 5 + 4 \times 3 + 8 \times 2 = 25 + 12 + 16 = 53 \text{ mm}$$

To allow for the serpentine flow, the PCB design incorporates one large semicircle at the top and two smaller semicircles at the bottom, as seen in Figure 8. The width of the magnet array, which is 53 mm, defines the diameter of the top semicircle. Therefore, the radius is calculated as:

$$R_{\text{top}} = \frac{53}{2} = 26.5 \text{ mm}$$

Each of the two smaller semicircles at the bottom spans a quarter of the array's width, so their radius is one-eighth of the total width.

$$R_{\text{bottom}} = \frac{53}{4} = 13.25 \text{ mm}$$

Therefore, the minimum height required to accommodate both the magnet array and serpentine trace layout is:

$$\text{Minimum height} = 50 + 26.5 + 13.25 = 89.75 \text{ mm}$$

To ensure sufficient clearance on the top and bottom, allowing space for screws, a 5 mm margin was added at both ends. This brought the total enclosure height to 100 mm. Moreover, a 10 mm margin was added to the left and right sides, increasing the total width to approximately 75 mm. These final dimensions were also used to define the overall shape and layout of the PCB design in the next section.

The enclosure will be 3D printed with PLA filament, since this method allows for accurate design whilst maintaining a lightweight enclosure, which is paramount to maintain comfort during long durations of use. Each driver will contain 18 magnets in total. The mass of each magnet can be calculated from its known density of 7.4 g/cm³:

$$\text{mass} = \rho \times \text{volume} = 7.4 \times 5 \times 0.5 \times 0.3 = 5.55 \text{ g} \quad (20)$$

According to Equation (20), each magnet has a mass of 5.55g, meaning the total mass of all magnets in one driver is approximately 100g. The mass of the drivers as a whole, including the screws, magnets, and the 3D printed enclosure, is 143g, therefore the headphones mass will be a minimum of 286g, excluding headband and ear padding. Estimating an additional mass of around 150-200g for these components, the final assembled weight is anticipated to be between 436-486g.

Even with these additions, the predicted headphone mass remains lighter than many commercial planar magnetic models, such as the Audeze LCD-X (592g) [17] or the HIFIMAN HE-6 (502g) [18], which demonstrates the viability of the proposed design.

4.2 PCB Design

The PCB was designed to ensure it's tracks aligned with the magnetic field loops produced by the magnet arrays, as shown in Figure 12. The first step in designing the PCB was to define its shape and determine where the traces should be routed. As established in the previous section, the face of the driver enclosure defined the outer boundary of the PCB, as illustrated in Figure 19.

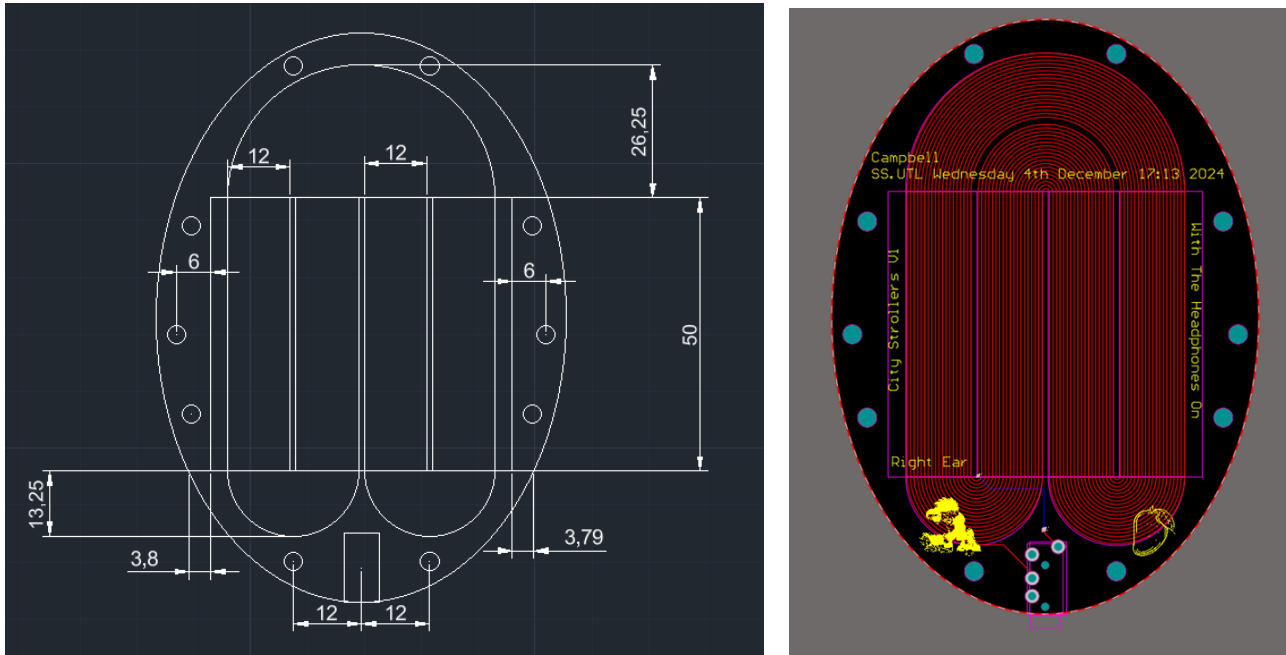
Alongside the outline, the mounting holes, each with a radius of 1.6 mm (designed for use with 3 mm screws), were carried over from the enclosure face. The small discrepancy of 0.1 mm between the screw and hole radius is intentional and essential; it allows the diaphragm to remain taut while preventing horizontal displacement when a force is applied perpendicular to its surface. These holes are symmetrically distributed around the board and maintain even tension across the diaphragm. This uniform tension ensures consistent mechanical behaviour and helps prevent local resonances.

Additional features were added to the face, including track outlines that serve as routing guides for the serpentine traces. These guidelines were based on the magnetic loop width of 12 mm, as defined

in Section 4.1, and were spaced across a 53 mm horizontal distance, and 50 mm height (from magnet height). The large semicircle at the top and two smaller semicircles at the bottom were also added.

This layout was exported from AutoCAD as a .dwg file and imported into Altium as a drawing on the mechanical layer (shown in purple in Figure 16b). With the track areas clearly defined and The University of Manchester's PCB fabrication constraints applied, the routing could begin.

Each track was routed from top to bottom of its assigned guideline, with 20 traces placed within each. This matched the earlier calculated maximum number of traces per magnetic loop, and therefore the resistance calculation remains the same as found in Section 4.1: 22.98Ω across the entire diaphragm.



(a) Driver enclosure outline used as a reference for PCB shape.

(b) Final PCB layout in Altium.

Fig. 16. PCB design progression from enclosure outline to fully routed PCB layout.

As justified in Section 3.2, a polyimide-based material is most suitable for this design due to its combination of flexibility, thermal stability, and mechanical durability. At The University of Manchester, the PCB printing facilities only permitted the use of Kapton, a widely used polyimide material meeting necessary requirements. While Kapton is not the lightest flexible PCB material available, it was the only material accessible within the scope of this project. Nevertheless, the magnetic force generated by the selected magnets (as shown in Section 4.1) is more than sufficient to maintain control over the diaphragm, even with the slightly increased mass.

With the material selected and the design finalised, fabrication could begin. However, challenges were encountered during the via production process due to facility limitations:

After a PCB's design has been etched and holes have been drilled, connectivity between the layers must be established. This is achieved using plated through-holes, or vias, created through a process

called electroplating. Electroplating involves passing an electric current through a solution known as an electrolyte, which contains copper ions. These ions are attracted to and deposit onto the exposed surfaces of the drilled holes, forming a conductive copper layer that connects different layers of the PCB [19]. This process is relatively straightforward for rigid boards, as they remain stable in the copper-based solution. However, flexible PCBs tend to sway in the solution, which can disrupt the plating process.

In large-scale manufacturing, specialised clamps are used to hold flexible PCBs in place, ensuring proper copper deposition inside the vias. However, due to limitations in the university's facilities, the PCB could not be adequately clamped, preventing the copper from plating inside the vias and resulting in open circuits. To resolve this, a thin piece of conductor had to be manually fed through each via and soldered on both sides to restore connectivity.



(a) Inspecting the printed circuit board via.



(b) Creating connectivity between layers on flexible PCB.

Fig. 17. Soldering process: inspection (left) and connection creation (right).

With connectivity complete, the final step was to assemble the device and test the performance of the drivers.

The assembly process involved enclosing the drivers shown in Figure 15b within a 3D-printed earcup and attaching ear pads and a headband. The earcup was designed in AutoCAD, and a key design decision was made regarding its acoustic structure. Headphone enclosures typically fall into two main categories: open-back and closed-back. Closed-back designs trap air within the earcup, meaning that diaphragm movement compresses and decompresses this enclosed air with each push or pull. This increases damping on the diaphragm, requiring more power to drive and reducing overall efficiency. Additionally, if the sound waves cannot escape, they reflect off the enclosure walls and interfere with

each other, either constructively or destructively, affecting the sound perceived at the ear. This effect is more prominent at lower frequencies, as their longer wavelengths are more difficult to absorb. The result is low-frequency buildup and resonances, which is why closed-back headphones tend to have a more prominent bass response [21].

While this may enhance certain listening experiences, it introduces colouration to the audio, which contradicts the aim of this project: to deliver a clean and accurate reproduction of the original signal while minimising distortion. Therefore, an open-back design was chosen. Open-back enclosures allow air and sound to pass freely through the earcup, significantly reducing internal reflections and resulting in a more transparent and natural sound.



(a) Front of planar magnetic headphones side.

(b) Back of planar magnetic headphones side.

Fig. 18. Full build of planar magnetic headphones.

Once fully assembled, the total weight of the headphones was measured to be 472g, making them lighter than many commercial planar models such as the Audeze LCD-X (592g) [17].

5 Experiment results

To evaluate the performance of the drivers, it is important to understand how their electrical characteristics behave across the audible frequency spectrum. This is paramount, since the perceived sound is directly related to the amplitude and consistency of the diaphragm's motion, which themselves are governed by both the voltage delivered and the electrical impedance of the driver. As explained in Section 3.1, the diaphragm's motion is driven by the force resulting from the interaction

between the current-carrying traces and the magnetic field, as described by Equation (2). Variations in voltage or impedance across frequencies affect the current delivered, which in turn alters the applied force and the system's transfer characteristics.

Additionally, as discussed in Section 3.2, the impedance of the diaphragm plays a critical role in determining the damping factor, defined as the ratio between load and source impedance. This factor influences the amplifier's ability to control the diaphragm, particularly following transients. To maintain consistent control, the load resistance should remain as flat as possible across the frequency range. To assess this, measurements of voltage and impedance across the headphone load were taken over a frequency sweep from 20 Hz to 20 kHz. These measurements provide frequency response plots that describe how the device responds to various input signals, forming a basis for understanding any deviations in acoustic performance across the frequency spectrum.

To establish a comparative reference, the same measurements were conducted on the Sony WH-1000XM3 headphones. This allows for a qualitative comparison and helps contextualise the performance of the developed drivers relative to a commercially optimised product using dynamic drivers. This comparison is directly aligned with the aim of the report: To determine if planar magnetic drivers can act as a competitive, high-performance alternative to dominant headphone technologies.



(a) Custom planar magnetic headphones.

(b) Sony XM3 headphones used as a reference [20].

Fig. 19. Comparison between custom headphones and XM3.

Each measurement was conducted twice at separate times to ensure consistency and repeatability. Minor variations may be present due to environmental conditions or manual setup, but the results shown represent the averaged and most consistent data obtained during testing, any more prominent

patterns or deviations will be analysed.

6 Discussion

To measure the voltage across the headphone load, a waveform generator was used. The waveform generator was configured to High-Z mode to minimise current draw and allow accurate voltage readings at the load. When the generator is connected in series with the headphone load, they form a voltage divider. By measuring the voltage at the headphone terminals, the portion of the input voltage dropped across the load can be determined. A 1 V_{pp} sine wave was used for all tests, as this closely matches the output level of typical consumer DACs, such as those found in smartphones like the iPhone, making the measurements more representative of real-world operating conditions.

6.1 Planar Magnetic Headphone (Custom System)

The first test will measure the variation in voltage across the load throughout the entire audible frequency range.

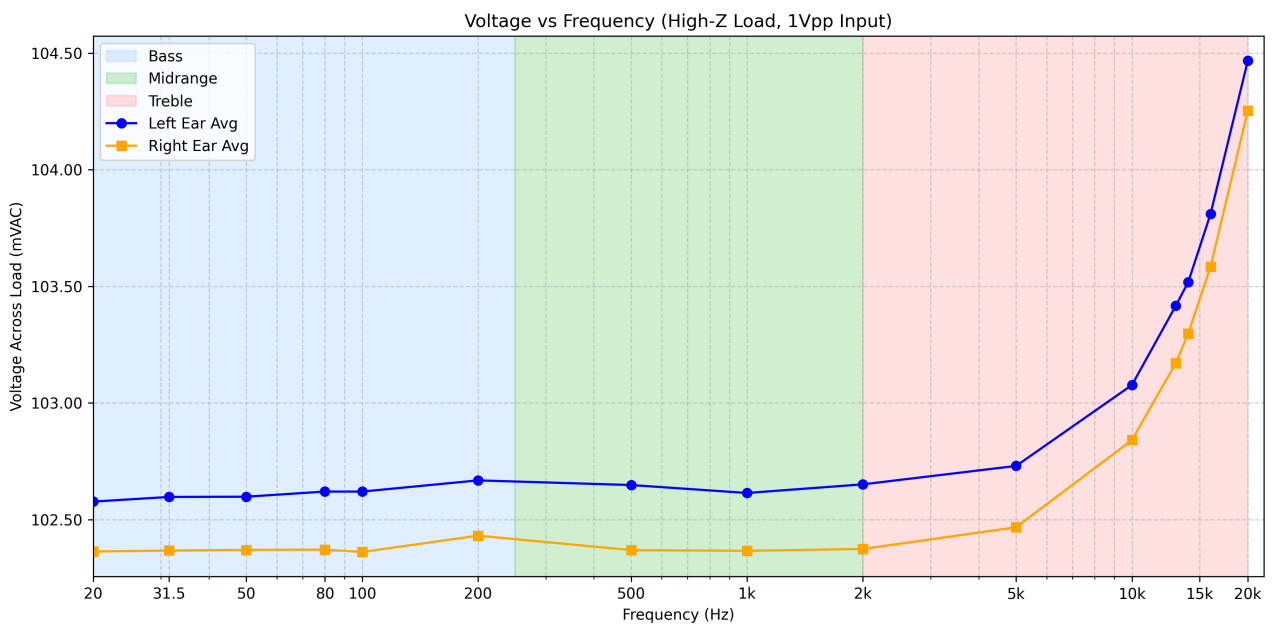


Fig. 20. Voltage response vs frequency using a high impedance source.

From Figure 20, it is evident that the right and left ears follow a closely matched pattern, with a slight discrepancy: the left ear exhibits a higher average voltage across all frequencies. Through the bass and mid-range, both drivers show a relatively flat voltage load, indicating consistent performance. However, as the frequency increases into the treble range, a rise in voltage is observed. Although this rise appears pronounced visually, the actual variation is subtle. The maximum fluctuation from the signal's minimum at 20 Hz to its maximum at 20 kHz is only 1.89mV for either ear. This small fluctuation in applied voltage across the frequency spectrum implies a consistent force on

the diaphragm over most of the audible range, a behaviour consistent with expectations outlined in Section 4.2, which predicted steady voltage and current due to a predominantly resistive load.

The left ear consistently exhibits a slightly higher average voltage than the right, suggesting a minor variation in load characteristics between the two channels. Assuming the amplifier provides a relatively balanced current to both ears, the higher voltage observed on the left could indicate a proportionally higher impedance, though this cannot be confirmed until impedance is directly measured in the following section.

To measure the impedance of the headphone load, an LCR meter was used. This instrument applies a small AC test signal across the load and directly measures the resulting voltage and current to calculate impedance at various frequencies. Unlike the waveform generator setup, the LCR meter is designed specifically for impedance characterisation, providing more accurate and frequency-dependent measurements of both resistive and reactive components. This facilitates a clearer understanding of how the headphone load behaves across the frequency spectrum.

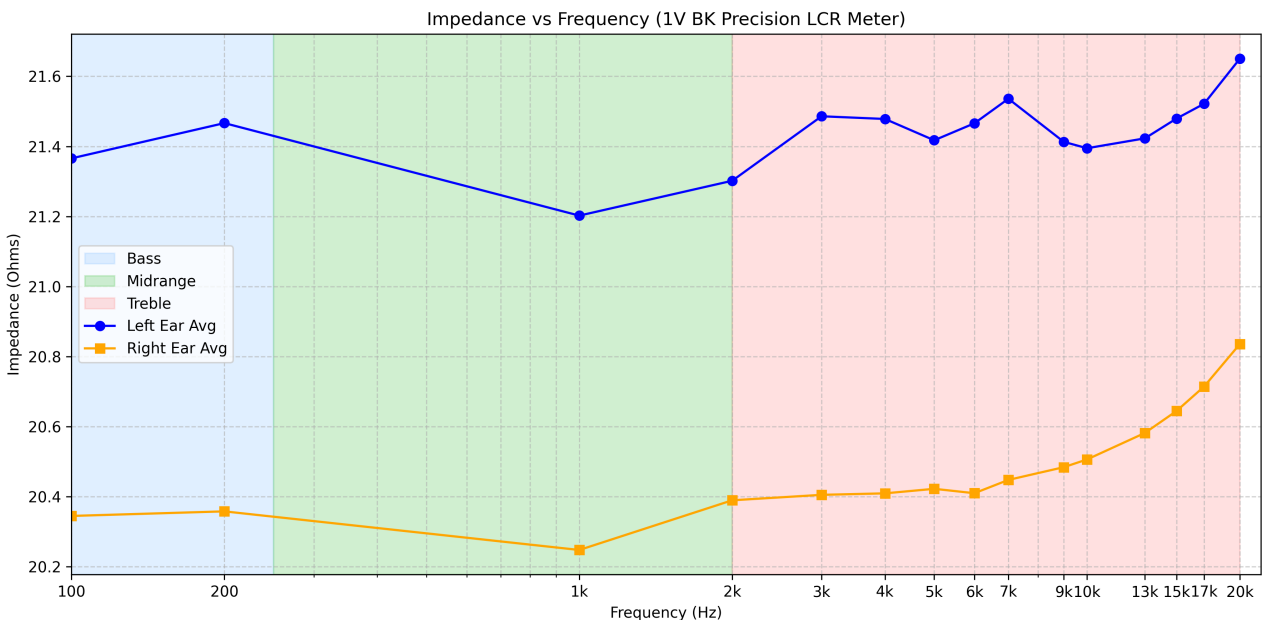


Fig. 21. Impedance response vs frequency for left and right drivers.

From Figure 21, the average impedance of the left ear is consistently higher than that of the right ear, as anticipated previously; however, both follow a similar shape. Both channels remain relatively flat across the bass and mid-range frequencies, similarly to the voltage response plot, indicating a predominantly resistive load. The most notable feature appears in the treble region, where impedance begins to rise slightly with frequency, more noticeably for the right ear. This rise in impedance is due to inductive effects at higher frequencies. The PCB's serpentine design creates a large loop area and therefore inductance is introduced. Inductive reactance (X_L) is proportional to frequency (f), as given by the equation:

$$X_L = 2\pi f L \quad (21)$$

Referring to Equation 21, as frequency increases, the inductive reactance also increases, contributing to the observed rise in impedance. Nevertheless, it is important to note that this rise is relatively small, approximately 0.6 Ω at most for both ears. The cause of this impedance increase can be further verified by plotting the phase angle over frequency. The phase of a signal indicates the relative timing between the voltage and current of the load.

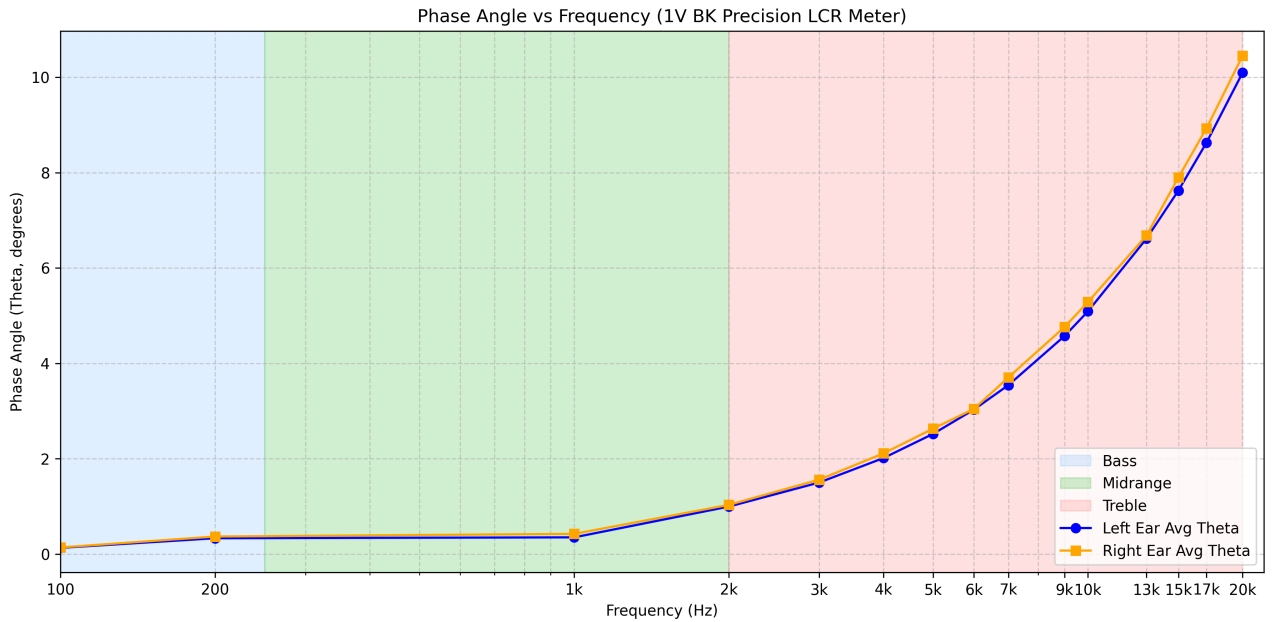


Fig. 22. Phase angle response showing inductive behaviour at higher frequencies.

A phase angle of 0° indicates no lag between voltage and current, which is characteristic of a purely resistive load. This behaviour is observed up to approximately 1 kHz, after which the phase angle gradually begins to increase. A positive phase angle means that current lags behind voltage, indicating inductive behaviour. As frequency increases beyond the midrange, the phase angle rises more noticeably, following an exponential trend. This trend aligns with the previous voltage and impedance plots and further illustrates that the impedance increase is caused by inductive effects in the PCB trace layout.

The initial flat response of the graphs suggests a tightly controlled diaphragm receiving consistent voltage and current, allowing the amplifier to manage its movement effectively. However, as frequency increases into the treble range, a steep rise in inductive effects becomes evident. This corresponds to increased impedance, meaning less current flows for the same voltage. As a result, the diaphragm experiences reduced force at these frequencies, according to Equation (2), making it more loosely controlled. This leads to a loss of clarity at higher frequencies, with sound becoming more smeared and less detailed.

6.2 Sony WH-1000XM3 Benchmark Comparison

The same tests were carried out on an industry-approved headphone, the Sony XM3s, creating a basis for comparison for the planar magnetic implementation:

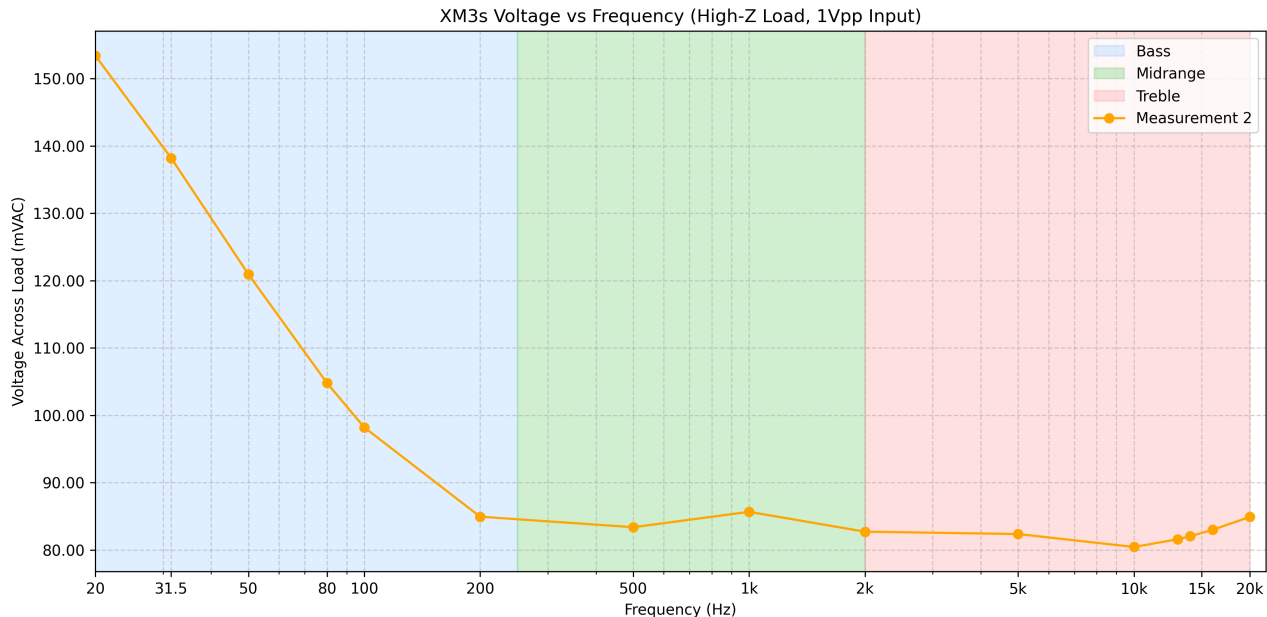


Fig. 23. Voltage vs Frequency Response for Sony XM3s.

Figure 23 shows a steep decrease in voltage across the bass range, dropping by 73 mV. This large discrepancy contrasts with the planar magnetic design, which exhibited only a 1.89 mV fluctuation across the entire frequency range. The magnitude of this drop suggests a significant impedance shift in the bass region, resulting in less voltage being applied across the headphone load. This behaviour could lead to a weakened bass response unless compensated for via DSP or EQ. In contrast, the planar magnetic design maintains near-constant voltage across the frequency spectrum, ensuring a more uniform force on the diaphragm and a more accurate reproduction of the input signal.

As the XM3s transition into the mid and treble ranges, the voltage response becomes flatter, though still shows a 4 mV variation. This is more than twice the total variation observed in the planar magnetic design, which exhibited a maximum discrepancy of only 1.89 mV across the entire 20 Hz to 20 kHz range. This suggests that the XM3s exhibit less linearity and may require active compensation to maintain balance across the spectrum.

Assuming a constant current source, the steep drop in voltage at low frequencies would indicate a corresponding drop in impedance. To test this assumption, the headphones' impedance was measured across the audible frequency range:

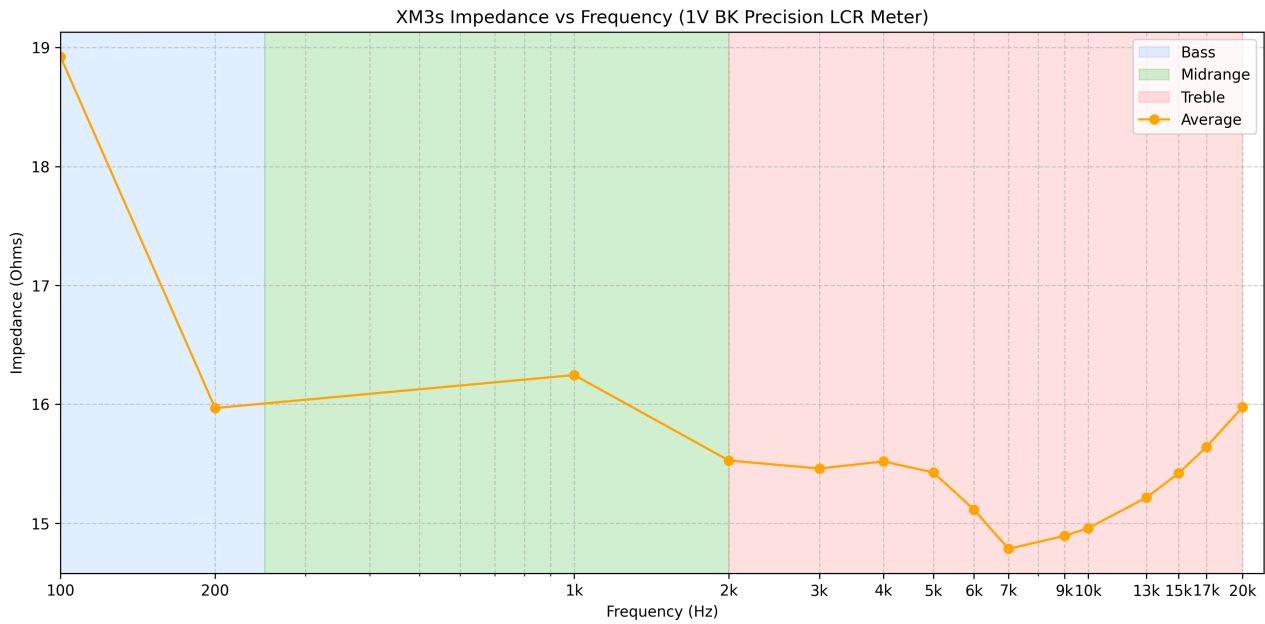


Fig. 24. Impedance vs Frequency Response for Sony XM3s.

As shown in Figure 24, the XM3s display a significant 3Ω drop in impedance within the bass range, which is five times the 0.6Ω change observed across the entirety of the frequency range for the planar magnetic drivers. This drop in the bass range aligns with the drop in voltage seen during the same region. The XM3's impedance becomes more linear into the midrange and early treble; however, they experience a further drop to 14Ω at 7 kHz, followed by a steep rise of 2Ω , peaking at 16Ω by 20 kHz. These fluctuations illustrate the inconsistency of this system and demonstrate a more difficult load for an amplifier to drive. In total, across the entire audible range, the largest variation in impedance across the XM3 load was from 19Ω to 14Ω , a difference of 5Ω , whereas for the planar magnetic implementation, the largest variation was 0.6Ω . This represents a reduction in impedance variation of 88%, indicating significantly more stable electrical characteristics

This behaviour reflects a less stable load across the frequency spectrum, particularly in the treble region where impedance increases rapidly. Such reactive characteristics challenge the amplifier's ability to deliver consistent current, especially at higher frequencies where impedance changes are most abrupt. In contrast, the planar drivers exhibit minimal variation, enabling tighter diaphragm control and more faithful signal reproduction. Varying impedance can cause the amplifier's voltage and current delivery to become uneven, potentially resulting in inaccuracies in sound reproduction.

To gain further insight into the cause of the impedance fluctuations, the phase angle was measured across the frequency range for the XM3s. The reactive nature of the headphones' load impedance, evident from its continuous variation with frequency, suggests that the phase angle should also vary continuously, rather than remain flat over a range, as observed in the custom planar headphone implementation shown in Figure 22.

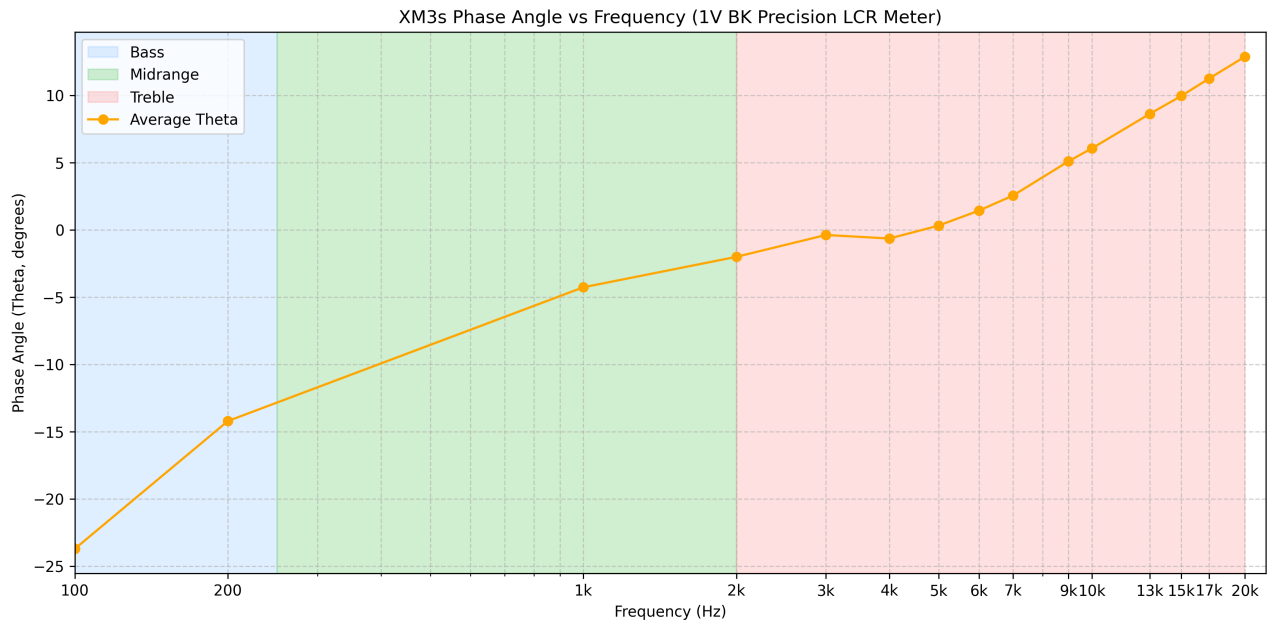


Fig. 25. Phase Angle vs Frequency for Sony XM3s.

From Figure 25, the phase angle shifts by 34° across the entire frequency range. The XM3 headphones exhibit capacitive characteristics up to 5 kHz, where current leads voltage, then shifts to inductive behaviour in the treble range, where current lags. In contrast, the planar design maintained a steady phase angle of 0° up to the treble range and only showed a relatively small 10° inductive shift. The XM3's impedance, however, fluctuates drastically across the frequency range, forming a complex and reactive load. From the driver's perspective, this makes it much harder to reproduce a reference signal accurately. The amplifier must constantly adapt to the changing load, causing the driver to receive a less direct and more delayed signal.

To conclude, the planar magnetic headphones demonstrated significantly better electrical performance compared to the Sony XM3s in terms of providing a consistent load and requiring a stable voltage. The planar implementation exhibited a minimal voltage variation of just 1.89 mV across the audible range, in contrast to the 73 mV observed in the XM3s. Additionally, the variation in load impedance was only 0.6Ω , compared to 5Ω . These differences reflect how easily the amplifier can control the load. The smaller fluctuations in load mean the amplifier maintains more stable control, resulting in less distortion and more accurate sound reproduction, as the force on the diaphragm stays consistent across the frequency range.

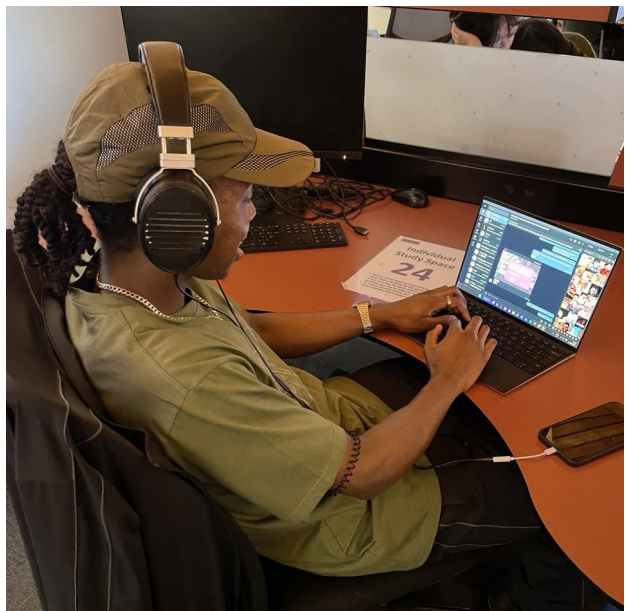
The relatively flat curves seen for the planar implementation in comparison to those in the XM3s suggest less distortion will be added to the input signal, which aligns with the aim of the project: to deliver a high sound quality with minimal distortion. To achieve this aim for XM3s however would require active correction using an equaliser, mean whilst the proposed planar magnetic implementation achieves it inherently through its consistent electrical characteristics, eliminating the

need for external processing.

7 Conclusion and Future Works



(a) Photo wearing the final assembled headphones.



(b) Testing headphones in a real-world use case.

Fig. 26. Demonstrating final design in use.

Overall, the drivers delivered strong performance, showing consistent load impedance and voltage across the diaphragm in the bass and midrange, resulting in clear, detailed sound and achieving the goal of accurate audio reproduction. Beyond electrical behaviour, the improvement over typical dynamic drivers also stemmed from the diaphragm material. While Kapton isn't as light as LCP, it offers low density and good flexibility, allowing fast, controlled movement. Combined with the evenly distributed force of the planar magnetic layout, this enables more accurate diaphragm motion and better transient response. In contrast, dynamic drivers rely on a single driving point and often use heavier diaphragm materials, resulting in uneven vibrations, resonances, and greater inertia.

Additionally, the improved sound quality did not come at the expense of weight, which is a common limitation of planar magnetic headphones. The final design weighed 472 g, significantly lighter than many competing planar models. This demonstrates the successful implementation of Halbach magnet arrays as an effective method for reducing weight while maintaining performance. Thus, the project successfully met its primary aim: delivering high sound quality while mitigating the typical weight disadvantage of planar magnetic headphones. That said, there are still areas for improvement.

It is evident that at higher frequencies, particularly in the treble region, there is reduced control over the diaphragm due to increases in load impedance. Less current flowing through the traces results in a weaker Lorentz force, leading to reduced diaphragm control compared to lower frequencies. This causes the signal to sound more blurred and less clear, as the amplifier struggles to quickly stop and

start the diaphragm in response to transients. While this issue was far more prominent in the dynamic drivers, it was still observable in the planar drivers and ultimately contributed to a less detailed treble response that was audible to the ear.

The impedance increase at higher frequencies was due to increased inductance, which aligns with expectations given the PCB design and its large loop area. For the next iteration, it would be ideal to reduce this inductance, potentially by implementing a combed PCB layout. In this arrangement, each outgoing current trace has a parallel return path, minimising the loop area and, therefore, the inductance. The return current flows in the same direction as the outgoing current within the magnetic field, so both experience force in the same direction. However, this setup presents challenges. It would require a current-mode amplifier with an output impedance significantly higher than that of the diaphragm, resulting in poor energy efficiency. Such amplifiers are also more complex to implement. While this layout could help reduce the inductance observed in the treble range, it introduces substantial practical drawbacks. Ideally, a winding arrangement should be developed that retains the benefits of a multi-turn layout while also minimising self-inductance.

In addition to this issue, it must be acknowledged that sound quality was also limited by the materials available at the University. In future iterations, a lighter diaphragm substrate such as aluminium-coated LCP, should be considered. This would reduce diaphragm inertia and enable tighter control over its motion, improving transient response and overall clarity.

While several planar magnetic headphone projects have been proposed, such as Apple's patented design [5], seldom have any completed real-world implementations supported by testing to validate their performance and viability in the market. Similarly, DIY efforts found in this space stop short of providing full characterisation and analysis to justify their claims. In contrast, this project provides a validated, fully functional system with quantifiable performance gains over a commercial benchmark. As such, it helps fill a gap in both academic and hobbyist-level work, offering a reference point for future research and development in compact planar driver systems.

This project demonstrated that planar magnetic drivers, when combined with Halbach arrays and an optimised PCB layout, can overcome both their own limitations and those of other driver types. The final prototype delivered accurate, consistent sound while remaining lighter than many competing planar models. These results confirm its viability as a high-performance alternative, meeting the goals of sound quality, efficiency, and portability.

References

- [1] Planar Magnetic Technology. (2014). *Planar Magnetic Technology White Paper*. Available at: https://theheadphonelist.com/wp-content/uploads/2014/06/pm_white-paper.pdf [Accessed 1 Apr. 2025].
- [2] C. Menges, "Headphone Driver Types Explained," *Moon Audio*, 2024. [Online]. Available: <https://www.moon-audio.com/blogs/expert-advice/headphone-driver-technology?fastr=true>. [Accessed: Apr. 09, 2025].
- [3] S. Hu, "Planar Magnetic Drivers: A Comprehensive Guide," *HiFiGo*, Jun. 28, 2023. [Online]. Available: <https://hifigo.com/blogs/guide/planar-magnetic-drivers>
- [4] "Halbach Arrays: The Ingenious Magnetic Arrangement You Need to Know About," *Stanford Magnets*, [Online]. Available: <https://www.stanfordmagnets.com/halbach-arrays-the-ingenious-magnetic-arrangement-you-need-to-know-about.html>
- [5] Apple Inc. (2015). *Planar Magnetic Transducer Systems*. U.S. Patent No. 9,208,697 B2. Available at: <https://patents.google.com/patent/US9942663B1> [Accessed 1 Apr. 2025].
- [6] Wikipedia Contributors, "Loudspeaker," *Wikipedia*, Oct. 31, 2019. [Online]. Available: <https://en.wikipedia.org/wiki/Loudspeaker>
- [7] Beyerdynamic, "Spotlight on Our Headphones: 87 Years of Headphones Expertise," *Beyerdynamic Blog*, May 2, 2024. [Online]. Available: <https://blog-na.beyerdynamic.com/spotlight-on-our-headphones-87-years-of-headphones-expertise/>. [Accessed: Apr. 9, 2025].
- [8] Yawny (2024). *Headphone Driver Types Explained: Dynamic, Planar, and More*. [online] [headphone.shop/](https://headphone.shop/headphone-driver-types-explained-dynamic-planar-and-more/) [Accessed 1 Apr. 2025].
- [9] "Electrostatic loudspeaker," *Wikipedia*, Jul. 09, 2020. [Online]. Available: https://en.wikipedia.org/wiki/Electrostatic_loudspeaker. [Accessed: Apr. 09, 2025].
- [10] "Planar Magnetic vs. Dynamic Drivers?," *Apos Audio*, [Online]. Available: <https://apos.audio/blogs/news/planar-magnetic-vs-dynamic>. [Accessed: Apr. 09, 2025].
- [11] The Physics Classroom (2019). *Sound Waves as Pressure Waves*. [online] Available at: <https://www.physicsclassroom.com/class/sound/u11l1c.cfm>.
- [12] "Damping Factor Explained," *KEF US*, [Online]. Available: <https://us.kef.com/blogs/news/damping-factor-explained>. [Accessed: Apr. 09, 2025].

- [13] MCL (2017). *What is the Difference between FR4 and Polyimide PCB.* [online] Available at: <https://www.mclpcb.com/blog/polyimide-pcb-material-information-fr4-vs-polyimide-pcb/>.
- [14] Magnet Source (n.d.). *Magnet Material Comparison Guide.* [online] Available at: <https://www.magnetsource.com/pages/product-comparison> and <https://online.fliphtml5.com/klhyq/nnyd/#p=1>.
- [15] Kjmagnetics.com. (2025). *Neodymium vs Ceramic Magnets | K&J Magnetics Blog.* [online] Available at: <https://www.kjmagnetics.com/blog/neodymium-vs-ceramic-magnets>.
- [16] Bunting-Berkhamsted. (2025). *Explaining Neodymium Magnet Strength.* [online] Available at: <https://www.bunting-berkhamsted.com/explaining-neodymium-magnet-strength/>.
- [17] Audeze LLC, “LCD-X,” *Audeze.* [Online]. Available: <https://www.audeze.com/products/lcd-x>. [Accessed: Apr. 09, 2025].
- [18] “Headphones & portable audio - HIFIMAN.com,” *HIFIMAN*, 2018. [Online]. Available: <https://www.hifiman.com/products/detail/75>. [Accessed: Apr. 09, 2025].
- [19] E. McMahon, “PCB Wrap Plating: Critical Process In Circuit Board Manufacturing,” *Epectec.com*, 2024. [Online]. Available: <https://blog.epectec.com/pcb-wrap-plating-critical-process-in-circuit-board-manufacturing>. [Accessed: Apr. 09, 2025].
- [20] “WH1000XM3B.CE7 | Buy WH-1000XM3 Wireless Noise Cancelling Headphones & View Price | Sony United Kingdom,” *Sony.co.uk*, 2024. [Online]. Available: <https://www.sony.co.uk/electronics/headband-headphones/wh-1000xm3/buy/wh1000xm3b.ce7>. [Accessed: Apr. 10, 2025].
- [21] C. Thomas, “Open back vs closed back headphones: which are right for you?,” *SoundGuys*, Apr. 20, 2017. [Online]. Available: <https://www.soundguys.com/open-back-vs-closed-back-headphones-12179/>
- [22] Q. S. Team, “Halbach array,” *QuickField.com*, Oct. 2020. [Online]. Available: https://quickfield.com/advanced/halbach_array.htm. [Accessed: Apr. 11, 2025].

A Appendices

A.1 Project Outline

Project Title

An Investigation into Halbach-Based Planar Magnetic Drivers as a Viable Alternative to Traditional Headphone Designs

Project Aim

To explore whether a novel implementation of planar magnetic drivers, specifically using a Halbach magnet array, can not only overcome the limitations of other driver technologies, but also address its own known shortcomings, offering accurate sound reproduction without compromising portability and weight.

Objectives

1. **Magnet Design:** Simulate and evaluate different magnet configurations (e.g., Halbach arrays) to maximise field strength and uniformity while minimising weight.
2. **Diaphragm Design:** Select a suitable PCB material and optimise its trace layout.
3. **Driver Construction:** Fabricate and assemble the drivers using 3D-printed enclosures and neodymium magnets in the chosen Halbach configuration.
4. **Electrical Characterisation:** Measure and analyse impedance and voltage response across the audible frequency range to assess the output signal integrity.
5. **Benchmark Comparison:** Compare the custom design to a commercial dynamic driver headphone (Sony WH-1000XM3) to evaluate improvements in impedance stability and signal linearity.

Expected Deliverables

- Fully functional planar magnetic headphone prototype
- Frequency response and impedance analysis plots
- Comparative study against a commercial benchmark
- Final dissertation with detailed theoretical and experimental findings, drawing a conclusion to what the project aimed to investigate.

Success Criteria

- Demonstrated impedance stability across the frequency spectrum
- Demonstrated reduction in weight compared to competing planar magnetic headphones
- Measured performance improvements over dynamic driver benchmarks
- Functional, wearable prototype with clear, distortion-free audio output
- Feasibility for real-world, portable headphone applications

A.2 Initial Project Plan

Scope and Objectives

The scope of this project is to design and build a pair of planar magnetic headphones with the following key features:

1. **Planar Magnetic Drivers:** Implement planar magnetic drivers to achieve high-quality sound reproduction with low distortion and detailed audio.
2. **Magnetic Driver Enclosure:** Fabricate a 3D-printed magnetic driver enclosure to support and align the magnet arrays.
3. **Bluetooth Audio Receiver:** Integrate a Bluetooth module to enable wireless audio transmission.
4. **Rechargeable Li-Po Battery:** Incorporate a rechargeable Li-Po battery to power the Bluetooth receiver and drivers.
5. **Push-Button Controls:** Devise a push-button interface for functions such as power control and Bluetooth pairing.

This project will focus on successfully integrating these features to create a functional and high-performing headphone system.

Deliverables

- Find the best magnet configuration to produce a strong and uniform magnetic field
- Design a flexible PCB for use as the diaphragm and current-carrying trace platform

- Create speaker units, including a 3D-printed driver enclosure
- Drive speaker units with a test signal to evaluate electrical and acoustic performance
- Implement and integrate a Bluetooth receiver to wirelessly drive the speaker units

A.3 Risk Register

Project Risk	Severity			Potential			Score (Severity x Potential) L=1, M=2, H=3	Mitigation Measures
	L	M	H	L	M	H		
Magnet snapping or damage during assembly	x			x			2	Wear glasses, use gloves, non-metal tweezers, and place magnets slowly
Burn hazard from soldering PCB manually			x	x			3	Wear heat-resistant gloves; ensure ventilation and focus
Back/neck pain from poor posture	x			x			1	Sit upright; adjust monitor height; take movement breaks

Fig. 27. Enter Caption

A.4 Continued Professional Development

Current and recent CPD activity:

CPD Activity Title	Description	Dates	CPD Hours
Give the CPD activity a title...	Describe the activity in brief...	When did the activity happen...	How many hours of learning do you think you gained for the activity...
YouTube Videos	Watching YouTube videos on headphone ratings and how sound quality is measured	04/02/2025	10+
PCB Design Course	Enrolled and completed with Altium PCB design course for PCB layout and trace optimization	15/02/2025	10
FEMM Simulation	Learning to simulate and analyse magnetic fields in 2D using FEMM	20/02/2025	5

Planned and Future CPD activity:

CPD Activity Title	Description	Skills addressed	Dates
Name of the CPD activity...	Describe the activity in brief...	What skills will the CPD activity enhance, or what skills-gap you have identified will it address...	When will this happen...
Audio Testing & Measurement	Learning how to use measurement rigs to assess frequency and distortion responses	Understand sound testing methods for audio products	20/04/2025
Technical Article Writing	Writing and publishing a technical article on planar magnetic headphone design	Develop written communication and publication skills	10/05/2025

Fig. 28. Continuing Professional Development Log

A.5 Health & Safety Risk Assessment

Activity	Hazard	Who might be harmed and how	Existing measures to control risk	Risk rating	Result
Preparing for the MEng Teaching Space	Students not familiar with emergency evacuation, 1st aid and general information about practical class	Staff, students Students not aware of the controls in place may put themselves or others in unnecessary danger	1. Lead Academic to provide induction prior to work commencing. 2. Lead Academic must ensure the MEng students are competent to work in the space including delivering the following information <ul style="list-style-type: none"> a. The most appropriate evacuation routes from the space b. Location of assembly point outside the building c. Clarify to the students if the fire alarm testing will occur during the class d. If student feels unwell or require first aid they must alert staff as soon as possible e. Location of 1st aid notices in the building f. Location of 1st aid boxes and eyewash g. Location of welfare facilities h. Appropriate dress code (PPE, no shorts or short skirts, hair tied up) i. No eating or drinking j. Must follow instructions at all time, no horseplay 	Low	A
	Students new to lab environment	Staff, students Students not aware of the controls in place may put themselves or others in unnecessary danger	1. Students are not allowed to work lone work in the lab and must always be in the space with at least 1 other person. 2. They must never attempt the work if not sure and always ask for help. 3. Academic lead must ensure MEng students are trained and competent to support the class. 4. Students must be provided with appropriate PPE according to the specific risk assessment 5. Students should be told of basic lab hygiene and good laboratory practices E.g. No eating & drinking, correct gloves removal technique, wash hands before leaving lab etc. 6. After class, students must tidy up, collect all their belongings and leave the lab in good condition 7. All students have completed a Department H&S induction 8. All students have completed the FSE Health and Safety Course on blackboard 9. All students have completed the MECD Health and Safety Courses on blackboard	Low	A

Activity	Hazard	Who might be harmed and how	Existing measures to control risk	Risk rating	Result
General working in the teaching laboratory	Slips, Trips and falls	Staff, students Strains and impact injuries	1. Floors and walkways kept clear of items, e.g. boxes, packaging, equipment etc 2. Furniture is arranged such that movement of people and equipment are not restricted. 3. No running in the spaces 4. Drawers and cabinets kept closed. 5. Walkways to be kept clear of trailing cables, bags to be stored under desk or in the lockers provided. 6. Ensure floor remains dry and mop up any spill liquids. 7. Reasonable standards of housekeeping maintained. 8. Report damaged flooring to Academic supervisor who will report appropriately 9. Adequate lighting provided. 10. At least one member of staff to be present at all times during timetabled laboratory sessions	Low	A
	Building Security Suspicious people in and around campus	User and others in building Difficulty in contacting help/assistance	1. Ensure Swipe card is used to access building and must not allow anyone to tailgate 2. If you see any suspicious activities in and around the premises, get yourself to a safe place and call Campus Security immediately on 0161 3069966 3. Must not enter into any area unauthorised for lone working or out-of-hours 4. When entering and exiting the building, keep to well-lit areas and be extra vigilant of surroundings 5. Students encouraged to download the SafeZone app to quickly get in touch with Security team to call for assistance, whether it's for a first aid incident or in an emergency. 6. Students to use SafeZone app to check-in which alerts security if you don't check-out.	Med	A

Activity	Hazard	Who might be harmed and how	Existing measures to control risk	Risk rating	Result
	Out of hours and lone working	User Difficulty in contacting help/assistance	<ol style="list-style-type: none"> No working out of hours allowed and only work within the MEng spaces can take place between 9am-5pm Monday to Friday Students are not allowed to work alone work in the MEng teaching spaces and must always be in the space with at least 1 other person. At least once a day, 1 project supervisor will do a spot check on the MEng spaces Students will have access to their project supervisor 9am-5pm via teams Students will have access to local support within the YSB if required. Students will log themselves into the space using an online spreadsheet Carry a charged up mobile phone on person at all times. Be aware of security contact telephone numbers, evacuation and first aid information indicated above. 	Med	A
Regular computer use	Poor posture, repetitive movements, long periods looking at DSE (display screen equipment)	Staff, students, visitors Back strain (due to poor posture). Repetitive Strain Injury (RSI) to upper limbs. Eye strain.	<ol style="list-style-type: none"> Please refer to the DSE policy, guidance and poster for more information on how to set up your workstation properly Complete DSE self-assessment for guidance on how to set up workstation properly Set up workstation to a comfortable position with good lighting and natural light where possible Take regular breaks away from the screen, at least some activity at your workstation every 20mins and a 5 minute break from workstation every hour. Regularly stretch your arms, back, neck, wrists and hands to avoid repetitive strain injuries. Refer to workstation exercises here Set up a desktop working space where possible and try to avoid working on a laptop without a docking station 	Low	A
Use of equipment	Electricity	User and others in the area Can cause fire, burns or electric shock	<ol style="list-style-type: none"> User is trained and supervised until fully competent. Visual inspection of equipment for obvious defects Defective plugs, cables equipment etc reported for repair/replacement and taken out of use. Check for PAT sticker is valid Use equipment as per manufacturer's guide. Sufficient power sockets provided to reduce need for extension cables. Make sure wires and cables never make contact with liquid. If faulty stop use immediately and report it to a lab technician. Switch off and make safe after use. 	Med	A

Activity	Hazard	Who might be harmed and how	Existing measures to control risk	Risk rating	Result
Use of hand tools (like sharp / pointed tools, Scalpel blade)	Sharp cutting edges	Users /Others in proximity / Visitors Risk of cuts and puncture injuries	<ol style="list-style-type: none"> User is trained and supervised until fully competent. Only use the tool for the intended use. Pre-use check for any faults and remove from use if any found. Avoid use of 'open bladed' tools, e.g. use scissors instead of scalpels if possible. Make safe after each use, e.g. razor blades to be put in sharps bin after use, knives to be replaced into protective cover. Place in safe storage immediately after each use. Never leave cutting tools unattended. Do not place cutting tools too close to the edge of workstation to avoid falling off onto legs and feet Consider the use of cut resistant gloves Use safe cutting technique e.g. cut away from the body and away from the hands and fingers 	Med	A
Use of equipment with mechanical hazards	User wearing loose clothing or long hair	User /Others in proximity / Visitors Risk of entanglement	<ol style="list-style-type: none"> Training and supervision on the machinery until fully competent. Avoid loose clothing and loose jewellery. Long hair must be tied back. Users must wear lab coat, safety glasses BS EN 166 and cut resistant gloves BS EN 388. A conveniently positioned mushroom shaped emergency stop button or is present to quickly stop the machine in an emergency. Machinery turned off when not in use. 	Med	A
Moving /lifting large/heavy items (including furniture, PCs, stationary)	Moving heavy, large or cumbersome loads/object	Staff, students, visitors, cleaners Crush injuries, strains and sprains, bruising	<ol style="list-style-type: none"> Contact Technical Services Manager or University portage for moves of large and/or heavy furniture. Do not attempt lifting heavy items unless trained and experienced For lighter items (generally below 10kg although dependant on individual capabilities), perform kinetic lifting with feet apart, load held close to body and in front of operator. Perform good loading technique: check weight, centre of gravity, sharp edges, use stable position, bend knees not back, have a firm grip on load, keep load close to body, avoid twisting or stretching, avoid lifts above shoulders / below knees, move smoothly, avoid jerky movements Do not store large, heavy or cumbersome items at height (e.g. on high shelves or on top of cabinets/bookcases etc). 	Med	A

Activity	Hazard	Who might be harmed and how	Existing measures to control risk	Risk rating	Result
Manual soldering Creation of joints between wires or components using molten solder. The application requires the use of a hot (~370-420°C iron) usually mains powered.	Heat	User / Visitors / Occupants of neighbouring areas Minor burns to skin, fire	1. No soldering equipment should be left unattended while switched on and for a minute after switching off to allow to cool. 2. Anyone approaching soldering equipment should assume it is hot. 3. 0.11mm nitrile gloves can be worn to protect hands from spitting solder 4. Solder away from combustible and flammable material 5. When not in use, soldering irons must be stored in the stands provided. 6. Cold water or burn gel should be applied immediately to all soldering iron burns and first aider called to assist.	Low	A
	Colophony (e.g. rosin) based solders that cause asthma	All users in lab Risk of asthma from Colophony	1. The use of rosin-based solders and fluxes should be limited and require registration with occupational health by emailing the lab screen questionnaire to millochealth@manchester.ac.uk (ask the Safety Advisor for a copy) 2. The use of local fume extraction is required when using rosin-based fluxes; or when using alternative fluxes for more than a few minutes a day, according to HSE guidance 3. If using extraction, do not begin task unless you have confirmed that the equipment is working. Ensure Allianz inspection is up to date and that the extraction is used as close to the fume source as possible 4. Label bottles clearly and decontaminate work area regularly 5. Keep away from food and drink areas and wash hand before leaving the lab 6. Add solders and fluxes to labcup	Med	A
	All other solders	Risk of irritant to respiratory system			
	Solder pastes and fluxes	All users in lab Risk of allergic contact dermatitis	1. The use of solders and fluxes that cause allergic contact dermatitis should be limited and require registration with occupational health by emailing the lab screen questionnaire to millochealth@manchester.ac.uk (ask the Safety Advisor for a copy) 2. 0.11mm nitrile gloves should be worn to protect skin from contact 3. Label bottles clearly and decontaminate work area regularly 4. Keep away from food and drink areas and wash hand before leaving the lab 7. Add solders and fluxes to labcup	Med	A
	Lead based solder	All users in lab Lead poisoning, increased risk for pregnant / breastfeeding mothers.	1. Lead at work guidance states below 500°C the lead fume is controlled, soldering irons do not reach this temperature (max 420°C) 2. Keep away from food and drink areas and wash hands after use 3. Add solders and fluxes to labcup	Med	A

Activity	Hazard	Who might be harmed and how	Existing measures to control risk	Risk rating	Result
Test and measurement	Electrical	Users /Others in proximity / Visitors Electric shock	1. User is trained and supervised until fully competent 2. Specific risk assessment required for: a. >50 volts AC / >60 volts DC b. intentional connection to human tissue c. low impedance situation, e.g. wet conditions		
	Heat	User / Others in proximity / Visitors Minor burns, fire	1. User is trained and supervised until fully competent 2. Keep area tidy and free from combustible or flammable materials 3. Exercise caution on first power-up. Limit supply current to just above expected level. 4. Specific risk assessment required for circuits containing intentional heating elements and/or operating at >850°C 5. Consider signage to warn others of heat hazard above 850°C	Low	A
	Component ejection	User / Others in proximity / Visitors Minor burns, eye injury	1. User is trained and supervised until fully competent 2. Wear safety glasses 3. Exercise caution on first power-up. Check for reverse connection of electrolytic capacitors before energising the circuit. 4. Limit supply current to just above the expected level 5. Avoid close visual inspection of an unproven circuit during the first few minutes of operation	Low	A
Solvent-based cleaning	Chemicals with health affects and flammable	Users /Others in proximity / Visitors Health damage and fire risk	1. Without a chemical risk assessment specific to the room and activity, no liquid chemicals are to be used in MEng spaces. 2. Complete chemical risk assessment and follow controls identified such as PPE (labcoat , correct gloves, safety glasses), extraction, training, supervision, storage and disposal procedures. 3. Perform correct glove removal to ensure you don't touch the outer part of the glove 4. Use the minimum quantity necessary (always below 500ml, above which required flammable storage) and ensure containers are sealed when not in use and stored safely. 5. Ensure good workspace ventilation. 6. In case of spillage, remove all sources of ignition. Absorb with absorbent materials from the lab's hazardous spill kit. Safely collect spills into suitable container for chemical waste disposal.	Med	A

Fig. 29. Health & Safety Risk Assessment Visuals

A.6 Gantt Chart

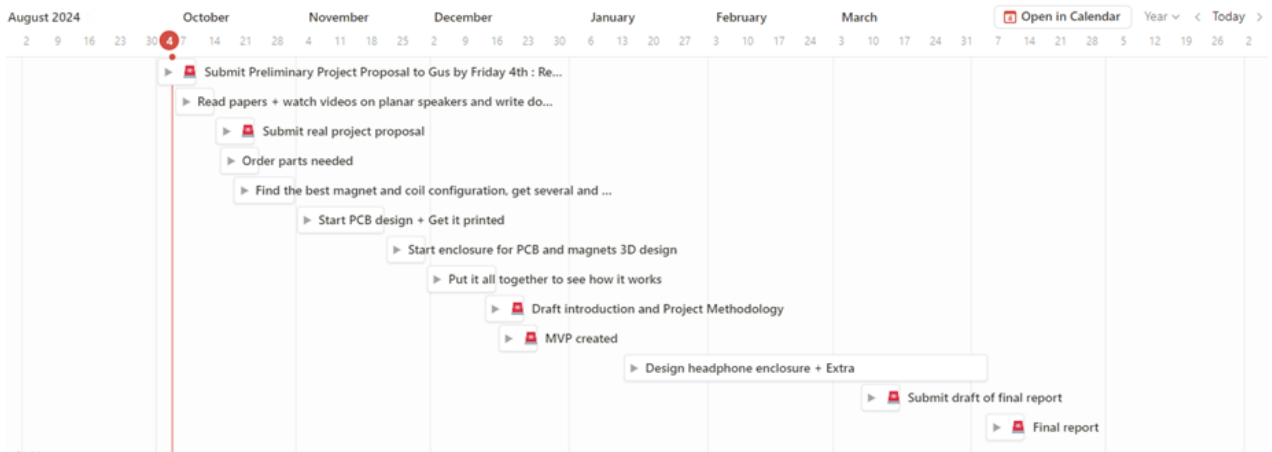


Fig. 30. Enter Caption

A.7 Source Code

Resistance Calculation Code (13 Traces)

The following Python code calculates the resistance for a serpentine PCB trace with 13 traces.

Listing 1. Python Code for Resistance Calculation

```
1 import math
2
3 total = 0
4
5 def calculateResistance(length_meters):
6     resistivity = 1.77e-8
7     width = 0.3e-3
8     thickness = 35e-6/2
9     return resistivity * length_meters / (width * thickness)
10
11 def calculateStraightSection():
12     # 4 tracks of 13 traces each, each 5 cm (0.05m) long
13     return 4 * 13 * calculateResistance(50e-3)
14
15 def calculateMiniCurvedSection():
16     mini_curve_total = 0
17     radius = 9.25e-3
18     for i in range(13):
19         mini_curve_total += (radius - (0.3e-3 * i)) * math.pi
20
21     return calculateResistance(3 * mini_curve_total)
22
```

```

23 def calculateMainCurvedSection():
24     main_curve_total = 0
25     radius = 18.5e-3
26     for i in range(13):
27         main_curve_total += (radius - (0.3e-3 * i)) * math.pi
28
29     return calculateResistance(main_curve_total)
30
31 total = calculateStraightSection() + calculateMiniCurvedSection()
32 + calculateMainCurvedSection()
33 print(total) # 14.14256806429124

```

Resistance Calculation Code (20 Traces)

The following Python code calculates the resistance for a serpentine PCB trace with 20 traces.

Listing 2. Python Code for Resistance Calculation

```

1 import numpy as np
2 import matplotlib.pyplot as plt
3
4 w_b = 12e-3
5 w_t = 0.3e-3
6 w_c = 0.3e-3
7
8 NoT = int(w_b / (w_t + w_c))
9
10 NoF = 2
11
12 h = 50e-3
13
14 NoPC = 32
15
16 NoP = 10000
17 X = np.zeros(NoP)
18 Y = np.zeros(NoP)
19
20 X[0] = 0
21 Y[0] = 0
22 pointer = 0
23
24 # Starting point is left bottom corner of the outmost turn
25 for i in range(1, NoT + 1):
26     for j in range(1, NoF + 1):

```

```

27     pointer += 1
28     X[pointer] = X[pointer - 1]
29     Y[pointer] = Y[pointer - 1] + h
30
31     radius = (NoT + 0.5 - i) * (w_t + w_c)
32     x_centre = X[pointer] + radius
33     y_centre = Y[pointer]
34
35     for k in range(1, NoPC // 2 + 1):
36         theta = np.pi - k * (2 * np.pi / NoPC)
37         pointer += 1
38         X[pointer] = x_centre + np.cos(theta) * radius
39         Y[pointer] = y_centre + np.sin(theta) * radius
40
41     pointer += 1
42     X[pointer] = X[pointer - 1]
43     Y[pointer] = Y[pointer - 1] - h
44
45     if j != NoF:
46         radius = (i - 0.5) * (w_t + w_c)
47         x_centre = X[pointer] + radius
48         y_centre = Y[pointer]
49
50         for k in range(1, NoPC // 2 + 1):
51             theta = np.pi + k * (2 * np.pi / NoPC)
52             pointer += 1
53             X[pointer] = x_centre + np.cos(theta) * radius
54             Y[pointer] = y_centre + np.sin(theta) * radius
55     else:
56         radius = w_b + (NoT + 0.5 - i) * (w_t + w_c)
57         x_centre = X[pointer] - radius
58         y_centre = Y[pointer]
59
60         for k in range(1, NoPC // 4 + 1):
61             theta = 0 - k * (2 * np.pi / NoPC)
62             pointer += 1
63             X[pointer] = x_centre + np.cos(theta) * radius
64             Y[pointer] = y_centre + np.sin(theta) * radius
65
66         pointer += 1
67         X[pointer] = X[pointer - 1] - (2 * (NoF - 2) * w_b) + (w_t + w_c)
68         Y[pointer] = Y[pointer - 1]
69
70         radius = w_b + (NoT + 0.5 - i) * (w_t + w_c)

```

```

71         x_centre = X[pointer]
72         y_centre = Y[pointer] + radius
73
74     for k in range(1, NoPC // 4 + 1):
75         theta = (-np.pi / 2) - k * (2 * np.pi / NoPC)
76         pointer += 1
77         X[pointer] = x_centre + np.cos(theta) * radius
78         Y[pointer] = y_centre + np.sin(theta) * radius
79
80 X = X[:pointer + 1]
81 Y = Y[:pointer + 1]
82
83 def calculate_trace_resistance(X, Y, resistivity=1.68e-8, trace_thickness=17.5e-6):
84     """
85     Calculate the resistance of the entire trace.
86
87     Parameters:
88     - X, Y: Arrays of x and y coordinates of the trace.
89     - resistivity: Electrical resistivity of the material  $\Omega(\text{m})$ , default is for copper.
90     - trace_thickness: Thickness of the trace (m), default is 35  $\mu\text{m}$  (typical PCB copper thickness).
91
92     Returns:
93     - Total resistance of the trace  $\Omega()$ .
94     """
95
95     total_length = np.sum(np.sqrt(np.diff(X)**2 + np.diff(Y)**2))
96     print(f"Computed trace length: {total_length:.3f} m")
97     cross_sectional_area = w_t * trace_thickness
98     resistance = resistivity * total_length / cross_sectional_area
99     return resistance
100
101 trace_resistance = calculate_trace_resistance(X, Y)
102 print(f"Total trace resistance: {trace_resistance:.6f} Ohms")
103
104 X_mm = X * 1000
105 Y_mm = Y * 1000
106
107 plt.figure()
108 plt.plot(X_mm, Y_mm)
109 plt.axis('equal')
110 plt.title("PCB Serpentine Trace Plot")
111 plt.xlabel("Width (mm)")
112 plt.ylabel("Height (mm)")
113 plt.xlim(0, 30)
114 plt.grid(True)

```

```
115 plt.show()
```

Serpentine PCB trace plotter

The following Python code visualise the serpentine PCB shape.

Listing 3. Python Code for Resistance Calculation

```
1 import math
2
3 total = 0
4
5 def calculateResistance(length_meters):
6     resistivity = 1.77e-8
7     width = 0.3e-3
8     thickness = 35e-6/2
9     return resistivity * length_meters / (width * thickness)
10
11 def calculateStraightSection():
12     return 4 * 20 * calculateResistance(50e-3)
13
14 def calculateMiniCurvedSection():
15     mini_curve_total = 0
16     radius = 12e-3
17     for i in range(20):
18         mini_curve_total += (radius - (0.3e-3 * i)) * math.pi
19
20     return calculateResistance(3 * mini_curve_total)
21
22 def calculateMainCurvedSection():
23     main_curve_total = 0
24     radius = 24e-3
25     for i in range(20):
26         main_curve_total += (radius - (0.3e-3 * i)) * math.pi
27
28     return calculateResistance(main_curve_total)
29
30 total = calculateStraightSection() + calculateMiniCurvedSection()
31 + calculateMainCurvedSection()
32 print(total) # 23.780803171318148
```

Magnetic Field Distribution Code

The following Python code calculates and visualizes the magnetic field distribution for multiple traces using the Biot-Savart Law.

Listing 4. Python Code for Resistance Calculation

```
1 import math
2
3 import numpy as np
4
5 import matplotlib.pyplot as plt
6
7
8 mu = 4 * math.pi * 1e-7 # Permeability of free space (T·m/A)
9
10
11 trace_spacing = 0.6
12 trace_count = 16
13
14
15 x_range = np.linspace(-2, trace_spacing * trace_count + 2, 200)
16 y_range = np.linspace(-5, 5, 200)
17 X, Y = np.meshgrid(x_range, y_range)
18
19
20 B_field = np.zeros(X.shape)
21
22
23 def BiotSavart_relative(radius):
24     if radius == 0:
25         return 0 # Avoid division by zero
26     return (mu) / (2 * math.pi * (radius / 1000)) # Convert mm to meters inside the function
27
28
29 def total_magnetic_field(X, Y, trace_count, trace_spacing):
30     B_total = np.zeros(X.shape) # Initialize total field
31
32     for i in range(trace_count):
33
34         # Assign x position of each trace, spaced by 0.6 mm
35         trace_position_x = i * trace_spacing
36
37         # Loop through all points in the grid
38         for row in range(X.shape[0]):
39
40             for col in range(X.shape[1]):
41
42                 # Compute the 2D distance from the trace to the grid point using Pythagoras
43                 radius = np.sqrt((X[row, col] - trace_position_x)**2 + (Y[row, col])**2)
44
45                 # Add the contribution of this trace to the total field at this point
46                 B_total[row, col] += BiotSavart_relative(radius)
47
48     return B_total
49
50
51
52 B_field = total_magnetic_field(X, Y, trace_count, trace_spacing)
53
54
55 plt.figure(figsize=(8, 6))
```

```
39 plt.contourf(X, Y, B_field, cmap='inferno')
40 plt.colorbar(label='Magnetic Field Strength (Relative)')
41
42 plt.yticks(np.arange(-4, 4.5, 0.5)) # Y-axis ticks from -4 mm to 4 mm, step of 0.5 mm
43
44 plt.title(f'Relative Magnetic Field Distribution for {trace_count} Traces (0.3mm Separation)')
45 plt.xlabel('Distance (mm)')
46 plt.ylabel('Height (mm)')
47 plt.grid(True)
48 plt.show()
```